

AD \_\_\_\_\_

Award Number: DAMD17-98-1-8611

TITLE: Natural History of Plexiform Neurofibromas in NF1

PRINCIPAL INVESTIGATOR: Bruce R. Korf, M.D., Ph.D.

CONTRACTING ORGANIZATION: University of Alabama at Birmingham  
Birmingham, AL 35242

REPORT DATE: October 2008

TYPE OF REPORT: Final Addendum

PREPARED FOR: U.S. Army Medical Research and Materiel Command  
Fort Detrick, Maryland 21702-5012

DISTRIBUTION STATEMENT:

x Approved for public release; distribution unlimited

The views, opinions and/or findings contained in this report are those of the author(s) and should not be construed as an official Department of the Army position, policy or decision unless so designated by other documentation.

# REPORT DOCUMENTATION PAGE

*Form Approved*  
*OMB No. 0704-0188*

Public reporting burden for this collection of information is estimated to average 1 hour per response, including the time for reviewing instructions, searching existing data sources, gathering and maintaining the data needed, and completing and reviewing this collection of information. Send comments regarding this burden estimate or any other aspect of this collection of information, including suggestions for reducing this burden to Department of Defense, Washington Headquarters Services, Directorate for Information Operations and Reports (0704-0188), 1215 Jefferson Davis Highway, Suite 1204, Arlington, VA 22202-4302. Respondents should be aware that notwithstanding any other provision of law, no person shall be subject to any penalty for failing to comply with a collection of information if it does not display a currently valid OMB control number. **PLEASE DO NOT RETURN YOUR FORM TO THE ABOVE ADDRESS.**

<b>1. REPORT DATE (DD-MM-YYYY)</b> 01-10-2008		<b>2. REPORT TYPE</b> Final Addendum		<b>3. DATES COVERED (From - To)</b> 1 Oct 1998 - 30 Sep 2008	
<b>4. TITLE AND SUBTITLE</b> Natural History of Plexiform Neurofibromas in NF1				<b>5a. CONTRACT NUMBER</b>	
				<b>5b. GRANT NUMBER</b> DAMD17-98-1-8611	
				<b>5c. PROGRAM ELEMENT NUMBER</b>	
<b>6. AUTHOR(S)</b> Bruce R. Korf, M.D., Ph.D. Email: bkorf.uab.edu				<b>5d. PROJECT NUMBER</b>	
				<b>5e. TASK NUMBER</b>	
				<b>5f. WORK UNIT NUMBER</b>	
<b>7. PERFORMING ORGANIZATION NAME(S) AND ADDRESS(ES)</b>  University of Alabama at Birmingham 1530 3 <sup>rd</sup> Ave. S. Kaul 230 Birmingham, AL 35242				<b>8. PERFORMING ORGANIZATION REPORT NUMBER</b>	
<b>9. SPONSORING / MONITORING AGENCY NAME(S) AND ADDRESS(ES)</b> U.S. Army Medical Research and Materiel Command Fort Detrick, MD 21702-5012				<b>10. SPONSOR/MONITOR'S ACRONYM(S)</b>	
				<b>11. SPONSOR/MONITOR'S REPORT NUMBER(S)</b>	
<b>12. DISTRIBUTION / AVAILABILITY STATEMENT</b> Approved for public release; distribution unlimited					
<b>13. SUPPLEMENTARY NOTES</b>					
<b>14. ABSTRACT</b> The overall goal of this study was to use volumetric MRI to define the natural history of untreated plexiform neurofibromas in patients with NF1. MRIs were obtained from patients with untreated plexiform neurofibromas and sent to a central location for volumetric analysis. Following the initial analysis using a manual method to delineate tumor boundaries, data were reanalyzed using two separate approaches to semi-automated analysis. Overall, most tumors, regardless of body site, remained stable in size during the course of study. There was a trend towards more rapid growth in younger patients, however. In addition, the imaging characteristics of superficial and abdominal plexiform neurofibromas have been described. The results have demonstrated that volumetric MRI provides a reproducible and practical approach to measurement of the growth of plexiform neurofibromas. This approach is now the standard approach in use to measure response of plexiform neurofibromas to therapy, including in the clinical trials being conducted by the NF Consortium.					
<b>15. SUBJECT TERMS</b> NF1, neurofibroma, plexiform, MRI, volumetric imaging					
<b>16. SECURITY CLASSIFICATION OF:</b>			<b>17. LIMITATION OF ABSTRACT</b>  UU	<b>18. NUMBER OF PAGES</b>  38	<b>19a. NAME OF RESPONSIBLE PERSON</b>
<b>a. REPORT</b> U	<b>b. ABSTRACT</b> U	<b>c. THIS PAGE</b> U			<b>19b. TELEPHONE NUMBER (include area code)</b>

## Table of Contents

<b>Introduction.....</b>	<b>4</b>
<b>Body.....</b>	<b>4</b>
<b>Key Research Accomplishments.....</b>	<b>13</b>
<b>Reportable Outcomes.....</b>	<b>13</b>
<b>Conclusion.....</b>	<b>14</b>
<b>References.....</b>	<b>14</b>
<b>Appendices.....</b>	<b>15</b>

## INTRODUCTION

The overall aim of this study was to determine the rate of growth of untreated plexiform neurofibromas in patients with NF1 using volumetric MRI. MRIs were obtained from multiple sites around the world and transmitted to a central facility in Cambridge, MA (WorldCare), where volumetric analysis was done. Early in the project, a validation study was done to establish the reproducibility of volumetric analysis. This study was published in 2003; since that time volumetric analysis has been the “gold standard” for analysis of the growth rate of plexiform neurofibromas. This final report reviews the findings from the volumetric analysis. In the time since the project was initiated, new approaches to volumetric analysis have been introduced. In the final year of the project, the data were reanalyzed using two newer volumetric approaches, and these data will also be presented.

## BODY

### Progress Report for Statement of Work by Task

#### **Task 1. Complete development of study infrastructure – Months 1-6**

##### **a. IRB approval at all clinical sites**

All of the participating centers had active IRB approval for recruitment during the duration of the study. The study has been kept open at University of Alabama at Birmingham, National Cancer Institute, and Massachusetts General Hospital where the volumetric analysis has been done, in order to allow reconciliation of volumetric data and final analysis.

##### **b. Complete clinical data entry forms and test electronic transfer of clinical data**

Data entry forms were completed by the end of the first year, and have not changed.

##### **c. Organize package of materials for pathology review and tissue repository**

This task was completed by the end of the second year and has not changed.

##### **d. Set up listserv and website**

The study website was operational at [www.nfstudies.org](http://www.nfstudies.org), but since completion of recruitment and volumetric analysis it is no longer active.

##### **e. Test MRI data transfer**

All testing and data transfer are completed.

##### **f. Purchase workstation and prepare data entry forms at WorldCare.**

The workstation was purchased in November of 1998.

**g. Prepare project monitoring flow sheet.**

All data have been entered into a new database customized for the project using StudyTrax software.

**h. Prepare recruitment letters for study subjects**

All recruitment is completed.

**i. Publicize study to NF community**

Publicity about the study has ceased since recruitment was halted.

**Task 2. Recruitment of Study Subjects – Months 6-24**

**a. Centers contact prospective study subjects**

**b. Enrollment of study subjects**

**c. First MRI and clinical data received**

The status of recruitment is indicated in Table 1. As has been described in previous reports, recruitment was more problematic than expected, especially for adults. There are various reasons that participants did not complete the study; these included development of tumors requiring further treatment (surgery, radiation, chemotherapy) and participants who were lost to follow-up. Data analysis will be based on the set of patients who have completed the study.

Study Category	Number Recruited	Completed Study
Head & Neck < 18 Years old (group A)	65	43
Head & Neck > 18 Years old (group B)	27	13
Trunk & Extremity < 18 Years old (group C/E)	89	57
Trunk & Extremity > 18 Years old (group D/F)	81	48
Total	262	161

**Table 1.** Number of subjects recruited by study category.

**d. Review of clinical entry criteria**

This was completed in 2002 and is no longer relevant since the study is closed to recruitment.

**e. Test of inter-observer reproducibility of designation of tumor margins by MRI**

Results of this study were previously reported. A paper on this topic was published in the American Journal of Radiology. (*Interobserver Reproducibility of Volumetric MR Imaging Measurements of Plexiform Neurofibromas* Tina Young Poussaint, Diego Jaramillo, Yuchiao Chang, and Bruce Korf AJR 2003; 180: 419-423).

**Task 3. Data Acquisition and analysis – Months 13-42**

All of the MRI data was received at WorldCare, a medical imaging company in Cambridge, MA. WorldCare technologists completed the volumetric measurements and all were then reviewed by the study radiologists. WorldCare is no longer involved in the study, but all of the data have been transferred to University of Alabama at Birmingham, permitting us to verify volumetric measurements that were made as necessary. During the last year of the study, additional volumetric analysis was done by two groups. First, Dr. Brigitte Widemann at National Cancer Institute used a semi-automated method, which is now being used in volumetric analysis of plexiform neurofibromas in the NF Consortium for clinical trials. Second, Dr. Gordon Harris at Massachusetts General Hospital used another computer-based system to perform volumetric studies.

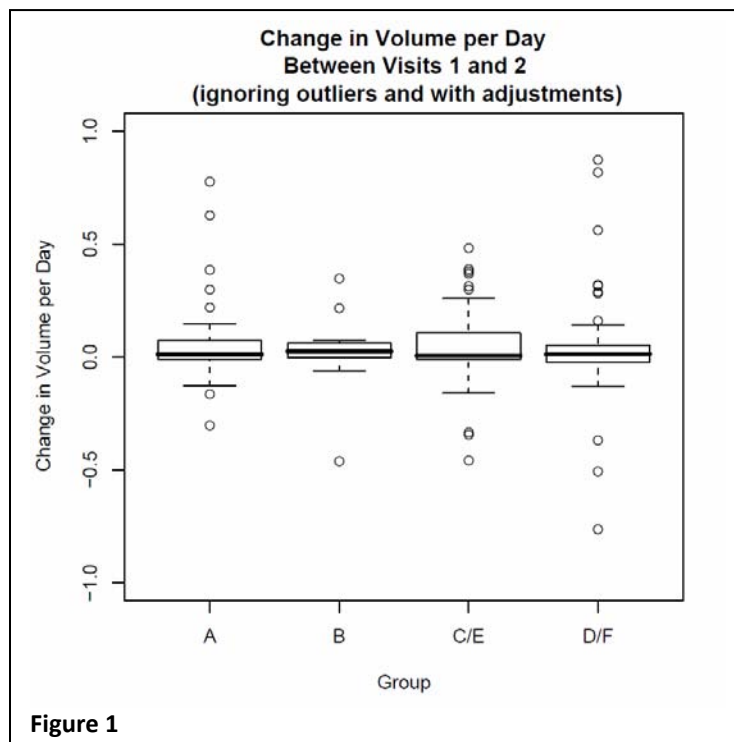
**a. Analysis of Data Using WorldCare Volumetric Approach**

For the analysis below, groups A, B, C/E, and D/F are defined in Table 1 on the previous page. Tumors with possible measurement errors were removed from analysis according to following cutoffs: change in volume per day: >1 mm/day; relative change in volume per day: >0.005 mm/day; exponential growth rate: >0.002 mm/day. In general, the WorldCare data do not show major trends in growth among the various tumor groups; in most cases growth rate differed little from 0, depending on the model used to assess growth (linear or exponential). There were, however, significant outliers in terms of growth in the various groups, indicating that most tumors did not grow during the study period, but there were notable exceptions.

**1. Change in tumor volume per day** were measured from volume of tumor and date of visit. This estimation of growth rate assumes that the growth rate of a tumor does not depend on volume. As shown in Table 2 and Figure 1 below, none of the groups shows a significant overall difference from 0, though there were tumors in each group that did show significant volume changes.

	N	Mean Change in Volume per day	Standard Deviation	Standard Error	95.0% Confidence Interval for Mean		Minimum	Maximum	Significance of Mean from Zero
					Lower Bound	Upper Bound			
<b>Group A</b>	42	0.056745	0.184024	0.028395	-0.0006013	0.114090308	-0.301835	0.775266	0.052338206
<b>Group B</b>	13	0.0194	0.181952	0.050465	-0.09055251	0.129353078	-0.461974	0.347599	0.707382768
<b>Groups C/E</b>	52	0.047128	0.17937	0.024874	-0.00280878	0.097065051	-0.456954	0.483853	0.063813206
<b>Groups D/F</b>	46	0.039516	0.264852	0.03905	-0.0391359	0.118166943	-0.763619	0.87174	0.316990176
<b>Total</b>	153	0.045123	0.208363	0.016845	0.011842297	0.078404106	-0.763619	0.87174	0.008204459

**Table 2.** Descriptive statistics for change in volume per day.

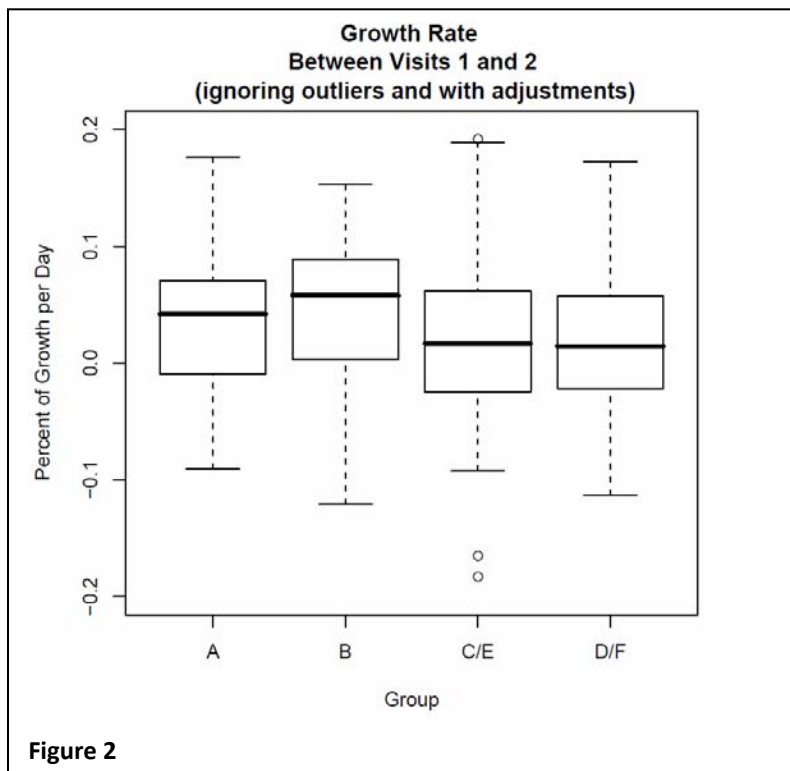


2. **Exponential Growth Rate** is estimated from volume of tumor and date of visit. This estimation of growth rate assumes an exponential growth rate.

	N	Mean Growth Rate	Standard Deviation	Standard Error	95.0% Confidence Interval for Mean		Minimum	Maximum	Significance of Mean from Zero
					Lower Bound	Upper Bound			
<b>Group A</b>	39	0.000355	0.000619	9.91E-05	0.000154731	0.000555781	-0.000903	0.001761	0.000942394
<b>Group B</b>	12	0.000427	0.000708	0.000204	-2.23E-05	0.000876967	-0.001209	0.001526	0.060462345
<b>Groups C/E</b>	55	0.000251	0.000812	0.00011	3.13E-05	0.00047046	-0.001831	0.00192	0.025894909
<b>Groups D/F</b>	47	0.000223	0.000735	0.000107	6.69E-06	0.000438448	-0.001134	0.001724	0.043579135
<b>Total</b>	153	0.000283	0.000731	5.91E-05	0.000165875	0.00039939	-0.001831	0.00192	4.06E-06

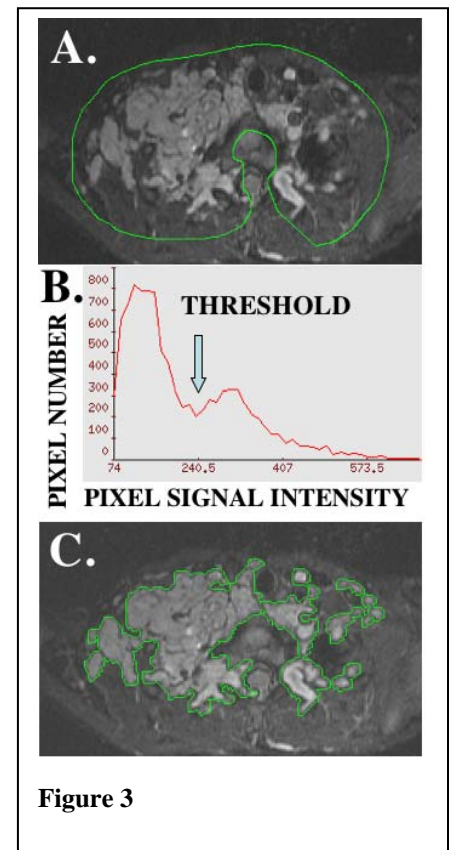
**Table 3.** Descriptive statistics for exponential growth rate per day of tumor.

Using the exponential model, all of the groups except for group B show a rate of growth different from 0.



## b. Analysis of Data using Alternative Volumetric Approach

The volumetric approach used by WorldCare was devised in the mid-1990s at the time when the project was first conceived. This approach was largely a manual one, in which a technologist selected a region of interest and needed to trace the outline of the tumor. Since that time, other approaches have been introduced that involve semi-automated analysis. The approach used at NCI has been adopted by the NF Consortium for use in measurement of plexiform neurofibromas in clinical trials, and therefore was an attractive approach to use to re-analyze the scans accumulated in this study. In addition, because it is based on an automated analysis, there is less likelihood of variation in delineation of tumor boundaries at different points in time as compared with the WorldCare approach. An additional analysis has been done by collaborators at Massachusetts General Hospital. These data are not presented here, however, as the analysis approach integrated all tumor visible within the field of imaging, whereas both the WorldCare and NCI analyses focused on a target region of interest. This makes the NCI and WorldCare analyses more comparable to one another. Of the 161 study subjects on whom two or more scans were available, 129 were provided to NCI for analysis. The scans that were not provided were those that existed only as film rather than DICOM images or where quality was not sufficient for analysis. The NCI method was described in publication (Computerized Medical Imaging and Graphics 2004 Jul; 28(5):257-65). The procedure is illustrated in Figure 3; it involves manual identification of a region of interest (the tumor) (Panel A), followed by automated histogram analysis of pixel signal intensity and identification of a threshold that separates tumor from other structures (Panel B), followed by automated re-drawing of tumor contours based on this threshold (Panel C). Areas are then measured in each slice and integrated over the length of the tumor to produce a volume.



The NCI analysis also included 60 plexiform neurofibromas from patients who were being treated on protocols at NCI from September 1999 through July 2007. These neurofibromas were not included in those that had been analyzed in this natural history study, and therefore the NCI study involved a comparison of these two groups (the natural history study group is referred to as the “UAB” group). The two study groups are described below:

NCI Group: NIH (n=60) - On-treatment patients (age 1.9 - 25 years) who had volumetric MRI analysis of their plexiform neurofibroma at the Pediatric Oncology Branch with at least 15 months follow up time between Sept 1999 and July 2007.

**NCI Group: (# of patients = 60), (# of MRI studies = 555)**

	<b>Age (yrs) at Entry</b>	<b>Initial Tumor Size (ml)</b>	<b>End of Study Tumor Size (ml)</b>	<b>Δ Tumor Size (%/yr)</b>	<b>Study Length (yrs)</b>
<b>median</b>	8.3	465	714.2	14.3	3.3
<b>max</b>	25.0	13.7	8448	115.8	7.2
<b>min</b>	1.9	13.7	25.1	-1.0	1.5

**Table 4.** Characteristics of patients in NCI cohort.

UAB Group: All patients were enrolled on a multi-institution NF1 natural history study. 129 patients had volumetric analysis of their plexiform neurofibromas.

**UAB Group: (# of patients = 129), (# of MRI studies = 428)**

	<b>Age (yrs) at Entry</b>	<b>Initial Tumor Size (ml)</b>	<b>End of Study Tumor Size (ml)</b>	<b>Δ Tumor Size (%/yr)</b>	<b>Study Length (yrs)</b>
<b>median</b>	13.7	187	215	6.84	2.0
<b>max</b>	55.5	21803	24360	58.9	6.4
<b>min</b>	2.5	3	4.9	--24	.2

**Table 5.** Characteristics of patients in UAB cohort.

For all patients, linear regression was used to obtain the slope of the % change in tumor volume relative to baseline. PN growth rate was plotted against the patient's age. The variation in PN growth rate by age group and distribution of PN growth rate was determined.

## A. Relationship of Age and Growth Rate

Although there was scatter of growth rate as a function of age, in both groups there was a correlation of age and growth rate, with younger patients having more rapidly growing tumors ( $R = 0.56808$ ).

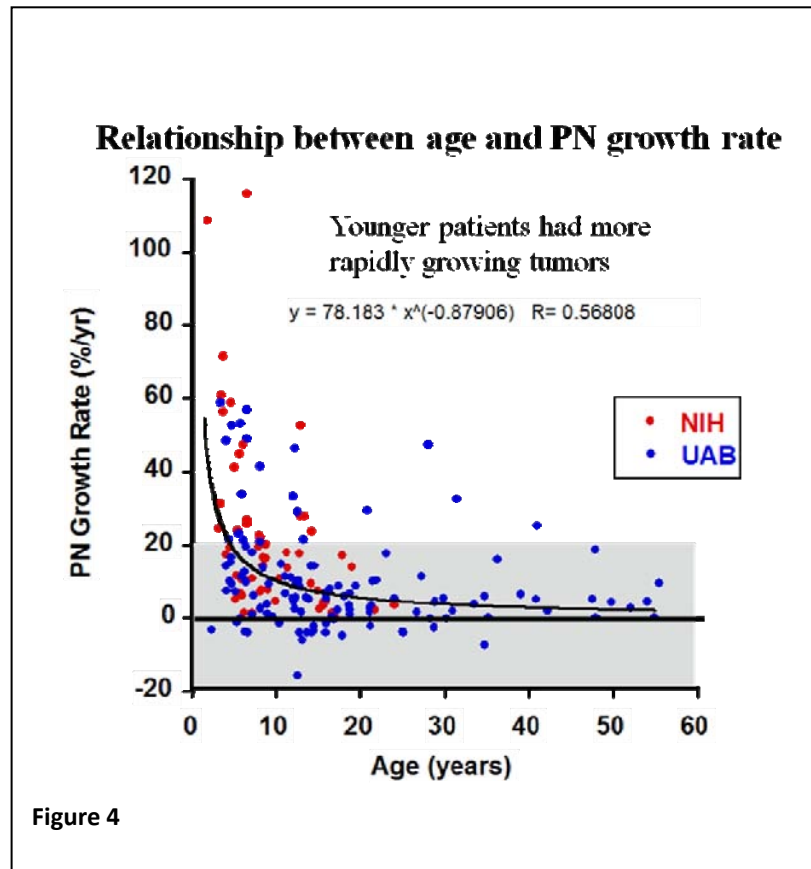
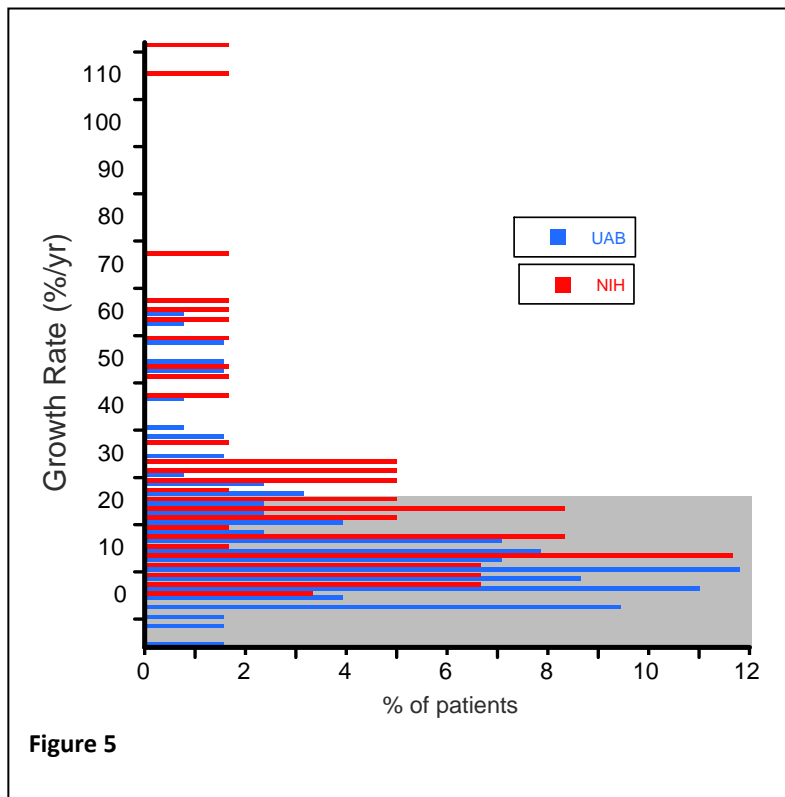


Figure 4

## B. Distribution of Plexiform Neurofibroma Growth Rate

Both the NCI patients and the UAB patients were found to have a low growth rate, in most cases less than 20% change in volume per year. This accords with the findings of the analysis of the WorldCare data. Most of the patients with a growth rate above 20% volume change per year were in the NCI cohort, as might be expected given that these were selected for treatment on the basis of significant symptoms or growth, whereas the UAB cohort were not selected for such characteristics.



### c. Imaging Characteristics of Plexiform Neurofibromas

In addition to study of the rate of growth of tumors, we have also analyzed imaging characteristics of plexiform neurofibromas. Two studies on this topic have been published; abstracts from each publication are reproduced below to summarize these findings.

#### 1. Superficial neurofibroma: A lesion with unique MRI characteristics in patients with NF1. (Lim R., Jaramillo D, Poussaint TY, Chang Y, Korf B. AJR 2005;184:962-968.)

**Objective:** Our aim was to test the hypothesis that in neurofibromatosis type 1 (NF1), superficial plexiform neurofibromas have different MRI characteristics than deep plexiform neurofibromas.

**Subjects and Methods:** Sixty-six patients (median age, 15 years) with superficial plexiform neurofibromas were compared with 56 patients with deep plexiform neurofibromas (median age, 12 years). All patients underwent axial STIR and coronal or sagittal STIR images.

**Results:** Superficial neurofibromas were more likely to be asymmetric ( $p = 0.004$ ) and extend to the skin surface ( $p < 0.001$ ). Lesion borders were poorly defined with similar frequency in both superficial and deep groups (77% vs 68%,  $p = 0.31$ ). The morphology of superficial neurofibromas was more likely diffuse (64% vs 11%,  $p < 0.001$ ), whereas deep neurofibromas were more likely nodular or fascicular. Of neurofibromas that were nodular or fascicular in morphology, superficial lesions had a smaller maximal fascicle–nodule diameter (mean, 10.3 mm) than deep lesions (mean, 13.4 mm) ( $p = 0.013$ ). Signal characteristics of deep neurofibromas were more likely to be targetlike (75%) compared with superficial neurofibromas (21%) ( $p < 0.001$ ). Superficial neurofibromas had a smaller mean volume than deep neurofibromas (180 vs 444 cm<sup>3</sup>,  $p = 0.002$ ).

**Conclusion:** Unlike the typical targetlike lesions along the course of major nerves seen in deep plexiform lesions, superficial plexiform neurofibromas in NF1 tend to be asymmetric, have nontargetlike signal intensity, lack nodular or fascicular morphology, and are likely to involve skin.

## **2. MR imaging of abdominopelvic involvement in neurofibromatosis type 1: A review of 43 patients. (Zacharia TT, Jaramillo D, Poussaint TY, Korf B. *Pediatr Radiol* 2005;35:317-322.).**

**Background:** Plexiform neurofibromas are a frequent complication of neurofibromatosis type 1. This article discusses MR imaging findings and distribution of plexiform neurofibromas in the abdomen and pelvis. Objective: To define the most prevalent patterns of involvement and MR imaging findings in abdominopelvic neurofibromatosis type 1. Materials and methods: We reviewed the MR appearance of abdominopelvic lesions in 23 male and 20 female patients (median age: 16 years) with type 1 neurofibromatosis. The patients were part of a multi-institutional study of 300 patients. Imaging included coronal or sagittal, and axial short tau inversion recovery images.

**Results:** The most common abdominopelvic involvement was in the abdominopelvic wall (n=28, 65%) and lumbosacral plexus (n=27, 63%). Retroperitoneal involvement was frequent (n=15, 35%). Lesions were less often intraperitoneal (21%) (P=0.001). Pelvic disease (n=27, 63%), neural canal involvement (n=18, 42%), and hydronephrosis (n=4, 9%) were also noted. Targetlike appearance of plexiform lesions was noted in more than half the patients.

**Conclusion:** Abdominopelvic involvement in neurofibromatosis type 1 is primarily extraperitoneal. Although lesions are most prevalent in the abdominopelvic wall and lumbosacral plexus, retroperitoneal and pelvic involvement is common and usually affects important organs. MR imaging added information in the initial and follow-up clinical evaluation of these patients.

## **KEY RESEARCH ACCOMPLISHMENTS**

- Publication of reproducibility study, demonstrating reliability of volumetric MRI approach. (*Interobserver Reproducibility of Volumetric MR Imaging Measurements of Plexiform Neurofibromas*. Tina Young Poussaint, Diego Jaramillo, Yuchiao Chang, and Bruce Korf *AJR* 2003; 180: 419-423)
- Publication of two papers on imaging characteristics of plexiform neurofibromas.
- Publication of study of growth rate of plexiform neurofibromas using NCI volumetric analysis technique; a second paper detailing the complete analysis of the UAB data analyzed by the NCI method is in preparation
- Establishment of volumetric MRI as the “gold standard” for clinical trials involving plexiform neurofibromas

## **REPORTABLE OUTCOMES**

1. Manuscripts: see references.
2. Presentations: Work has been presented in platform presentations and posters at the NF Conference and in an intramural conference at the National Cancer Institute.

3. Patents, licenses: none
4. Degrees obtained: not applicable
5. Tissue Repositories: A repository of blood and tumor tissue is now established at Washington University, St. Louis. This repository was initiated as part of this project, but is now being used by other treatment protocols as well.
6. Informatics: The NF International Database was modified to accommodate the specialized data collection required for use in this project. More recently all study data was transferred to a new database using the StudyTrax system.
7. Employment/research opportunities: not applicable

## **CONCLUSION**

The major outcome of this study has been the establishment of volumetric MRI as the standard approach to measurement of plexiform neurofibroma growth in clinical trials. This approach is now being used by the NF Consortium in clinical trials. We have also established that most plexiform neurofibromas grow slowly, if at all, and that growth rates tend to be greater in children than in adults. Finally, we have found that there are notable imaging differences between superficial and deeper plexiform neurofibromas. The biological basis for these differences has not been explored, but is open to further study.

## **REFERENCES**

- Young Poussaint T, Jaramillo D, Chang Y, Korf, B. Interobserver Reproducibility of Volumetric MR Imaging Measurements of Plexiform Neurofibromas. *American Journal of Radiology*. 2003;180:419-423.
- Korf, B. Determination of end points for treatment of neurofibromatosis 1. *J Child Neurol*. 2002 Aug;17(8):642-5.
- Lim R, Jaramillo D, Poussaint TY, Chang Y, Korf B. Superficial Neurofibroma: A Lesion With Unique MR Characteristics In Patients With Neurofibromatosis Type 1. *AJR Am.J.Roentgenol*. 2005;184(3):962.
- Zacharia TT, Jaramillo D, Poussaint TY, Korf B. MR Imaging of Abdominopelvic Involvement in Neurofibromatosis Type 1: A Review of 43 patients. *Pediatr.Radiol*. 2005;35(3):317.
- Dombi E, Solomon J, Gillespie AJ, Fox E, Balis FM, Patronas N, Korf BR, Babovic-Vuksanovic D, Packer RJ, Belasco J, Goldman S, Jakacki R, Kiern M, Steinberg SM, Widemann BC. NF1 plexiform neurofibroma growth rate by volumetric MRI. *Neurol* 2007;68:643-647.

## APPENDICES

Tina Young Poussaint<sup>1</sup>  
Diego Jaramillo<sup>2</sup>  
Yuchiao Chang<sup>3</sup>  
Bruce Korf<sup>4</sup>

## Interobserver Reproducibility of Volumetric MR Imaging Measurements of Plexiform Neurofibromas

**OBJECTIVE.** This article validates the reproducibility of MR imaging volumetric measurements for evaluating the growth of plexiform neurofibromas in neurofibromatosis type 1.

**CONCLUSION.** Volumetric measurements of plexiform neurofibromas in neurofibromatosis 1 are reproducible.

**N**eurofibromatosis type 1 is an autosomal dominant disorder that affects approximately one in 4000 individuals [1]. The hallmark feature is the occurrence of benign nerve sheath tumors, neurofibromas. Other features include café-au-lait macules, skin-fold freckles, optic gliomas, iris hamartomas (Lisch nodules), skeletal dysplasias, and malignant peripheral nerve sheath tumors. Much of the morbidity of the disorder is associated with the neurofibromas. Cutaneous neurofibromas can be present in large numbers, causing cosmetic disfigurement. Plexiform neurofibromas, occurring in 25% of individuals with neurofibromatosis 1, are characterized by longitudinal neurofibroma growth along nerves and involve multiple fascicles and branches. Plexiform neurofibromas lead to disfigurement, overgrowth, nerve compression, and even malignancy. The only current treatment for plexiform neurofibromas is surgery, but surgical resection is usually difficult because lesions are large and infiltrative. Recurrence is therefore common [2, 3].

The cloning of the neurofibromatosis 1 gene has resulted in insights into pathogenesis that may ultimately lead to the development of nonsurgical therapies. The gene responsible for neurofibromatosis 1 encodes a protein referred to as “neurofibromin,” which functions

at least in part as a negative regulator of *ras* family GTPases [4]. Clinical trials that have been undertaken or are contemplated include the use of farnesyl protein transferase inhibitors, angiogenesis inhibitors, cytodifferentiating agents, and hormonal modulators [5, 6].

The high rate of morbidity associated with plexiform neurofibromas makes them a good target for nonsurgical therapies. However, major challenges in the determination of outcomes measurements will complicate these trials. Plexiform neurofibromas may grow erratically, exhibiting periods of rapid growth followed by spontaneous stabilization. Also, the lesions may be large and irregularly shaped, making it difficult to measure their size and to follow changes related to growth or shrinkage in response to treatment.

Given these challenges, and the likelihood that drugs will be available for clinical trial in the near future, we have organized a multicenter trial to determine the natural history of plexiform neurofibromas in neurofibromatosis 1 using volumetric MR imaging. The major goals of that study are, first, to validate volumetric MR imaging as a means of following the growth of plexiform neurofibromas, and second, to generate a body of normative data on the growth rate of plexiform neurofibromas in different regions of the body.

Received June 17, 2002; accepted after revision August 6, 2002.

Supported by contract DAMD 17-98-1-8611 from the United States Army Medical Research Command.

<sup>1</sup>Department of Radiology, Children's Hospital and Harvard Medical School, 300 Longwood Ave., Boston, MA 02115. Address correspondence to T. Y. Poussaint.

<sup>2</sup>Department of Radiology, Massachusetts General Hospital and Harvard Medical School, 32 Fruit St., Boston, MA 02114.

<sup>3</sup>Department of Medicine, Massachusetts General Hospital and Harvard Medical School, 50 Staniford St., 9th Floor, Boston, MA 02114.

<sup>4</sup>Harvard-Partners Center for Genetics and Genomics and Harvard Medical School, 77 Ave. Louis Pasteur, Boston, MA 02115.

AJR 2003;180:419–423

0361–803X/03/1802–419

© American Roentgen Ray Society

The validity of the volumetric analysis is critically dependent on the ability of an observer to reproducibly determine the margins of a tumor in an MR image. We have studied the interobserver correlation of three observers analyzing volumetric MR imaging data to determine the degree of interobserver variation in the measurement of plexiform neurofibromas and the factors influencing this variation.

**Materials and Methods**

*Study Description*

Our overall study of the natural history of plexiform neurofibromas involves the recruitment of 300 patients with neurofibromatosis 1, half of whom are children younger than 18 years and half of whom are adults, with plexiform neurofibromas of the head and neck or of the trunk and extremities. Serial MR imaging examinations are done at three times during a 3-year observation period: first, at enrollment; second, at 1 year after enrollment; and third, at 3 years after enrollment. None of the patients is undergoing treatment during this period. The MR imaging data are sent to a central location for volumetric analysis of the plexiform neurofibroma. The human research committees of the 14 participating institutions approved the study.

The initial part of this study was to compare the volumetric measurements of neurofibromas performed by two radiologists and by a technologist experienced in volumetric assessment of lesions. MR imaging studies of the first 12 consecutive patients recruited were reviewed. All patients had been diagnosed as having neurofibromatosis 1, with the diagnosis established according to clinical criteria. The lesions involved the head and neck ( $n = 5$ ), spine ( $n = 4$ ), and trunk or extremities ( $n = 3$ ).

*MR Imaging*

Because patients were referred as part of a multicenter study, the MR imaging units were of different makes and field strengths, with 35 magnets at 1.5 T and one magnet at 1.0 T. The parameters varied according to the area being examined and the extent of the lesion. Coil and field-of-view selection varied according to the location of the lesion. The protocol included coronal, sagittal, and contiguous axial short tau inversion recovery images (TR/TE, 6000/35; inversion time, 150 msec; echo-train length, 8). Axial images were used for volumetric measurements. Slice thickness was 4 mm for the head and neck, 5 mm for the spine, and 10 mm for the extremities. The extremities were imaged with a matrix of  $512 \times 160$  so that the entire lesion could be covered in a reasonably short time; the other anatomic areas were imaged with a  $256 \times 256$  matrix.

*Volumetric Analysis and Validation with Phantom*

The volumetric analysis was performed using Cheshire software (version 4.4; Parexel, Waltham, MA), a commercially available, Food and Drug Administration–approved and validated desktop visualization and analysis program.

Verification of the analysis was performed using a balloon phantom consisting of an elongated balloon filled with 350 mL of water that was wrapped around the lower extremity of an adult volunteer with the intent of simulating a sciatic nerve neurofibroma. This balloon phantom was scanned using axial fast spin-echo inversion recovery technique (6000/35; inversion time, 150 msec; echo-train length, 8). Volumetric measurement was obtained by the computer-assisted method only.

Digital MR images were imported directly to the workstation, or hard-copy images were digitized and imported. Measurements were performed manually. Volume measurements were performed with an Autosegmentation tool of the

Cheshire software that determines the best-guess edge of a lesion, based on pixel values, and creates a region of interest (ROI) around the object. On short tau inversion recovery images, neurofibromas are of high signal intensity, whereas solid structures in the body are of very low signal intensity. The segmentation tool therefore successfully identifies the margins of the neurofibromas in most instances. To use this tool, the user must click in the center of the object, drag until the entire circle lies outside the object, and then release the mouse to create the ROI. After the segmentation, the user may use any of the ROI-modifying tools, such as the Nudge tool of the software to adjust the ROI to perfectly outline the object. The Volume Statistics function is used to compute the volume for all areas containing a selected ROI. Standardization of window values is set for all observers between 500 and 600 and the level between 150 and 200.

The technologist was initially instructed by the radiologists on the MR imaging appearance and signal characteristics of neurofibromas, using examples different from the ones used in the evaluation. To perform the reproducibility study, the technologist measured the volume of the lesion on each slice using the Autosegmentation tool. Each radiologist then reviewed the automated measurements and made adjustments using the Nudge tool, according to her or his clinical assessment. The measurements of the two radiologists were made independently and without knowledge of the other's interpretation.

*Statistical Analysis*

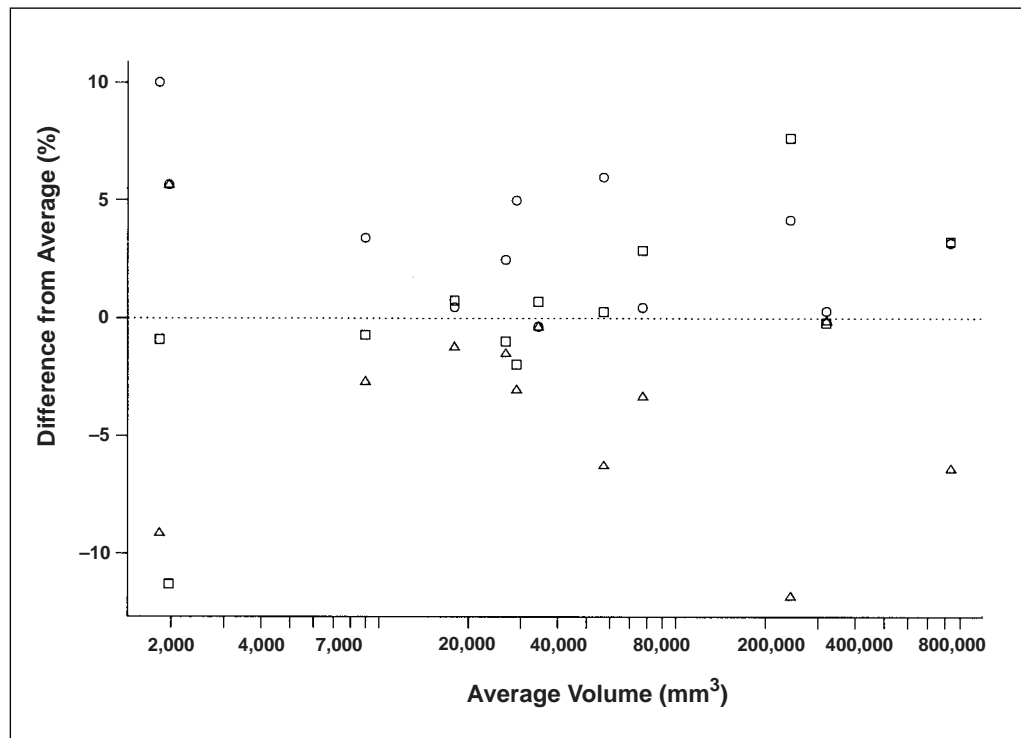
Interobserver reliability was assessed using the intraclass correlation coefficient, which is the proportion of total variability accounted for by the variability among subjects. If the intraclass correlation coefficient is high, then not much of the variability is due to variability in measurements from different raters [7].

<b>TABLE I Interobserver Variation for Volume Measurements</b>							
Patient	Area	Total Volume Data (mm <sup>3</sup> )			Deviance <sup>a</sup> (%)		
		Radiologist 1	Radiologist 2	Technologist	Radiologist 1	Radiologist 2	Technologist
1	Trunk or extremities	863,955	864,606	783,899	3.2	3.2	-6.4
2	Trunk or extremities	253,074	261,562	214,304	4.2	7.6	-12
3	Trunk or extremities	60,483	57,235	53,505	6.0	0.3	-6.3
4	Head and neck	18,023	18,073	17,722	0.5	0.7	-1.2
5	Head and neck	30,486	28,478	28,167	5.0	-1.9	-3.0
6	Spine	2,074	1,741	2,074	5.6	-11	5.6
7	Head and neck	77,669	79,522	74,754	0.5	2.9	-3.3
8	Head and neck	321,513	319,903	320,177	0.3	-0.2	-0.1
9	Head and neck	9,271	8,905	8,728	3.4	-0.7	-2.7
10	Spine	2,011	1,812	1,661	10	-0.9	-9.1
11	Spine	34,266	34,629	342,66	0.4	0.7	-0.4
12	Spine	27,351	26,436	26,299	2.5	-1.0	-1.5

<sup>a</sup>From average of three from each observer.

## MR Imaging Measurements of Plexiform Neurofibromas

**Fig. 1.**—Graph illustrates variation in volumetric measurements from mean among three observers. Volumes are graphed on logarithmic scale to show better variability by average volume. Most variation is less than 5% of mean volume. ○ = radiologist 1, □ = radiologist 2, △ = technologist.



### Results

When calibrated against a true volume of 350 mL, the results of the scan and volumetric analysis of the balloon phantom yielded a volume of 348 mL, which is equivalent to a measurement error of 0.6%.

The results of the measurements are summarized in Table 1 and in Figure 1. In Figure 1, the average of the three observers' measurements is taken as the standard, and deviations are recorded as a percentage of the total volume. As shown on the graph, the variability was usually less than 5%, and in all but two measurements, less than 10%. On the average, radiologist 1 measured a greater volume than the average, and the technologist measured the lowest volume. Measurements from radiologist 1 ranged from 3.2% lower to 19.1% higher than the measurements from radiologist 2 alone. The overall intraclass correlation coefficient was 0.996, which shows excellent agreement among raters. Stratified by group, the intraclass correlation coefficients for the head and neck and for the spine were both greater than 0.999. In Figures 2-4, plexiform neurofibromas in three representative locations are shown with the volumetric measurement outlined. The number of sections traced per patient depends on the size of the plexiform neurofibroma. Tracings were saved and recorded.

### Discussion

The study shows that interobserver variability in the volumetric measurement of MR images of plexiform neurofibromas is small.

Interobserver variability increases with increasing volume of the lesions, but volume measurements are generally within 10% of the mean of the measurements by three ob-

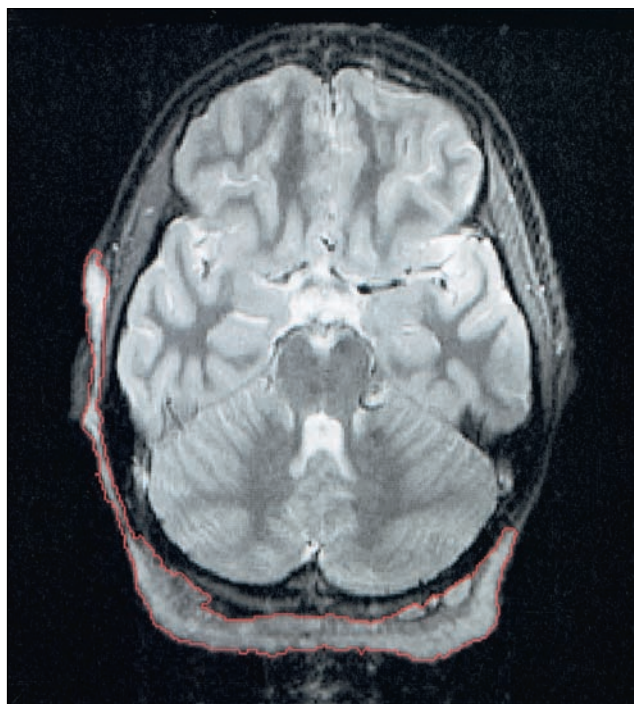


**Fig. 2.**—15-year-old girl with neurofibromatosis 1 and scalp mass. Axial fast spin-echo inversion recovery MR image shows lobulated scalp plexiform neurofibroma involving right temporalis muscle and suboccipital soft tissues. Volumetric measurements are outlined in red.

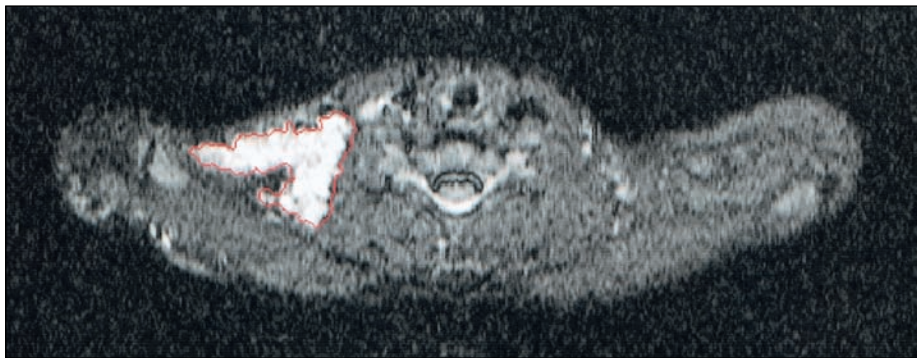


**Fig. 3.**—9-year-old girl with neurofibromatosis 1 and arm pain. Axial fast spin-echo inversion recovery MR image shows right brachial plexus lesion at level of lower cervical spine. Volumetric measurements are outlined in red.

servers. The technique of automatic preliminary volume determination followed by correction by the radiologist thus appears to be a reliable tool.

Determination of the rate of growth of plexiform neurofibromas will be important for selecting tumors appropriate for treatment in clinical trials and for measuring the outcomes of treatment. However, numerous difficulties are encountered in measuring plexiform neurofibromas. In each slice, the lesion may branch in many directions. Unlike most tumors, the borders of neurofibromas are ill defined, and their extension makes adequate lesion coverage challenging. For lesions that are diffuse, ill defined, and large, the time for measuring is longer. In some anatomic areas, it may be difficult to differentiate neurofibromas from normal structures. For example, bowel in the abdo-

men and pelvis, and lymph nodes in the head, neck, and mediastinum may resemble neurofibromas. Finally, neurofibromas may have different MR imaging appearances in various parts of the body. All these difficulties have created a lack of enthusiasm for or outright skepticism of the possibility of measuring tumor burden in neurofibromatosis 1. The semiautomatic segmentation technique in this study may allow quicker assessment of lesion volume than manual hand tracing.

Our strategy was based on two objectives: to maximize contrast between the lesions and the normal tissues; and to cover the entire lesion. Contrast maximization was best achieved using the short tau inversion recovery sequence with a long TR, which has been used for MR neurography [8, 9]. On long-TR, short tau inversion recovery images, most normal structures in the extremities,

head and neck, and spine are of low signal intensity, whereas neurofibromas are of high signal intensity. Slow-flowing vessels are usually indistinguishable from tumor, but we believe that they do not contribute substantially to tumor volume. The technique is less optimal when examining abdominal and pelvic structures because fluid-filled bowel can closely resemble neurofibromas. To cover the entire lesion, we used large fields of view, up to 10-mm slice thickness, and 160 phase-encoding steps, all of which allowed fast imaging, albeit at the expense of optimal image quality. This strategy will likely be equally reproducible in the evaluation of other complex tumoral lesions that have high signal intensity on short tau inversion recovery images.

Our data are limited by a relatively small sample size and the fact that the measurements of the radiologists were not done without their knowledge of the initial assessment by the technologist, which may bias the radiologists. We believe, however, that the major source of disagreement among observers lies with the determination of tumor versus nontumor on the MR images rather than with the identification of the initial area of interest. We do not have a means of determining the true volume of any of the tumors measured. Our data only address the degree of reproducibility in assessment of tumor volumes as determined by three observers. The data therefore reflect the precision but not the validity of the observations.

It remains to be shown whether the degree of reproducibility will allow detection of growth or shrinkage of plexiform neurofibromas based on serial MR imaging assessment. The current trial of a farnesyl transferase inhibitor, for example, defines progressive disease as an increase greater than or equal to 20% in the volume of the lesion. In this trial, the tumor contours are traced on each image

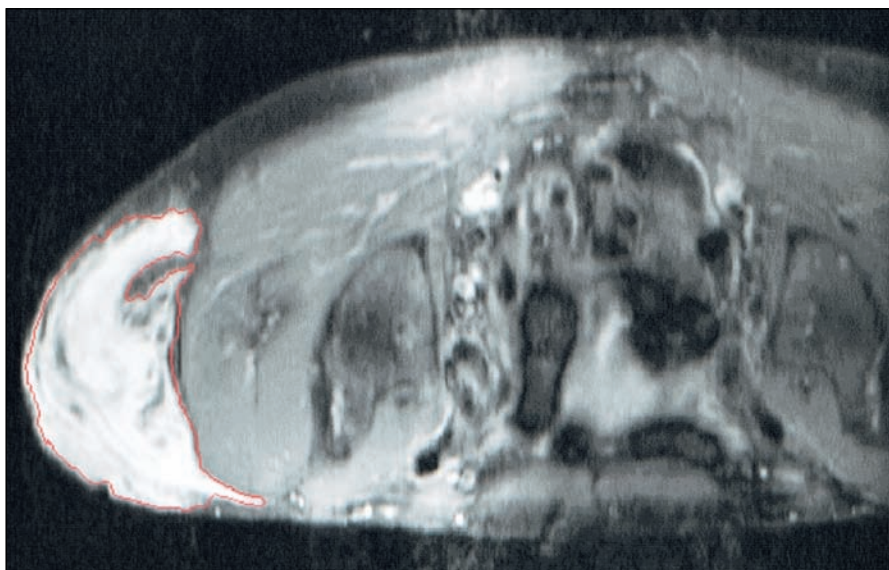


**Fig. 4.**—47-year-old woman with neurofibromatosis 1 and buttock mass. Axial fast spin-echo inversion recovery MR image obtained with patient in prone position shows large lesion involving subcutaneous tissues of gluteal region. Volumetric measurements are outlined in red.

## MR Imaging Measurements of Plexiform Neurofibromas

and volume is calculated by summing the results from all images based on the resulting two-dimensional contours and slice thickness. In the ongoing phase II trial, an automated method of tumor tracing for most of the tumors is used to determine the tumor volume. The interobserver variability, usually less than 5% and generally less than 10%, and the high interobserver correlations suggest that determination of volumetric change is feasible. We thus believe that reproducible computer-assisted volumetric analysis of plexiform neurofibromas can be performed successfully, and that such analysis may allow reliable assessment of changes in lesion volume.

### Acknowledgments

We thank Tara Flynn, project manager, and Erik Peterson and Noelle Sittkuhul of WorldCare, Inc., for help in performing volumetric measurements. We thank Virginia Grove for manuscript preparation.

### References

1. Huson SM. Recent developments in the diagnosis and management of neurofibromatosis. *Arch Dis Child* **1989**;64:745-749
2. Friedman JM, Gutmann DH, MacCollin M, Riccardi VM. Neurofibromatosis: phenotype, natural history, and pathogenesis, 3rd ed. Baltimore: Johns Hopkins Univ. Press, **1999**:142-161
3. Korf BR. Neurocutaneous syndromes: neurofibromatosis 1, neurofibromatosis 2, and tuberous sclerosis. *Curr Opin Neurol* **1997**;10:131-136
4. Korf BR. Plexiform neurofibromas. *Am J Med Genet* **1999**;89:31-37
5. Feldkamp MM, Gutmann DH, Guha A. Neurofibromatosis type 1: piecing the puzzle together. *Can J Neurol Sci* **1998**;25:181-191
6. Liebermann F, Korf BR. Emerging approaches toward the treatment of neurofibromatoses. *Genet Med* **1999**;1:158-164
7. Fleiss JL. Reliability of measurement. In: Fleiss JL, ed. *The design and analysis of clinical experiments*. New York: Wiley, **1986**:1-32
8. Moore KR, Tsuruda JS, Dailey AT. The value of MR neurography for evaluating extraspinal neuropathic leg pain: a pictorial essay. *AJNR* **2001**;22:786-794
9. Maravilla KR, Bowen BC. Imaging of the peripheral nervous system: evaluation of peripheral neuropathy and plexopathy. *AJNR* **1998**;19:1011-1023

The 2003 ARRS Annual Meeting will include a new issues forum on screening CT.

# Superficial Neurofibroma: A Lesion with Unique MRI Characteristics in Patients with Neurofibromatosis Type I

Ruth Lim<sup>1,2</sup>  
Diego Jaramillo<sup>3</sup>  
Tina Young Poussaint<sup>4</sup>  
Yuchiao Chang<sup>5</sup>  
Bruce Korf<sup>6</sup>

**OBJECTIVE.** Our aim was to test the hypothesis that in neurofibromatosis type 1 (NF1), superficial plexiform neurofibromas have different MRI characteristics than deep plexiform neurofibromas.

**SUBJECTS AND METHODS.** Sixty-six patients (median age, 15 years) with superficial plexiform neurofibromas were compared with 56 patients with deep plexiform neurofibromas (median age, 12 years). All patients underwent axial STIR and coronal or sagittal STIR images.

**RESULTS.** Superficial neurofibromas were more likely to be asymmetric ( $p = 0.004$ ) and extend to the skin surface ( $p < 0.001$ ). Lesion borders were poorly defined with similar frequency in both superficial and deep groups (77% vs 68%,  $p = 0.31$ ). The morphology of superficial neurofibromas was more likely diffuse (64% vs 11%,  $p < 0.001$ ), whereas deep neurofibromas were more likely nodular or fascicular. Of neurofibromas that were nodular or fascicular in morphology, superficial lesions had a smaller maximal fascicle-nodule diameter (mean, 10.3 mm) than deep lesions (mean, 13.4 mm) ( $p = 0.013$ ). Signal characteristics of deep neurofibromas were more likely to be targetlike (75%) compared with superficial neurofibromas (21%) ( $p < 0.001$ ). Superficial neurofibromas had a smaller mean volume than deep neurofibromas (180 vs 444 cm<sup>3</sup>,  $p = 0.002$ ).

**CONCLUSION.** Unlike the typical targetlike lesions along the course of major nerves seen in deep plexiform lesions, superficial plexiform neurofibromas in NF1 tend to be asymmetric, have nontargetlike signal intensity, lack nodular or fascicular morphology, and are likely to involve skin.

**A** characteristic feature of neurofibromatosis type 1 (NF1) is the occurrence of peripheral nerve sheath tumors, neurofibromas, which are the most common cause of symptoms and disfigurement in NF1 [1]. The term “plexiform neurofibroma” is used to describe a networklike growth of tumor involving multiple fascicles of a nerve, leading to a diffuse mass of thickened nerve fibers surrounded by proteinaceous matrix [1]. Plexiform neurofibromas can be deep or superficial in location or a combination of the two.

Plexiform neurofibromas often involve nerve plexuses, dorsal nerve roots, and other structures deep in relation to the muscle fascia and do not have any evident superficial extension. These deep lesions follow the course of major nerves. Past MRI studies have focused primarily on deep plexiform neurofibromas and show that they typically have a targetlike appearance on T2-weighted MR images, with

central low signal intensity and peripheral high signal intensity [1–4].

Other plexiform neurofibromas occur superficially and can be cutaneous or subcutaneous [1]. They can arise from peripheral nerves with no deep involvement, or they can represent superficial extension of a deeper plexiform neurofibroma [1]. Cutaneous involvement and subcutaneous involvement in NF1 are common. McLaughran et al. [5] investigated the clinical diagnostic features of NF1, including the prevalence of cutaneous and subcutaneous neurofibromas. They reported that well-circumscribed cutaneous neurofibromas were seen in 217 (59.5%) of 365 patients with NF1 and that 150 (45.5%) of 330 patients with NF1 had discrete subcutaneous neurofibromas. In addition, they found that 80 (15%) of 523 patients with NF1 had diffuse subcutaneous plexiform neurofibromas. Iannicelli et al. [6] found that in a group of 46 patients with NF1 with soft-tissue

Received April 2, 2004; accepted after revision July 20, 2004.

Supported by U.S. Army grant no. NF70002, “Natural History of Plexiform Neurofibromas in NF1.”

<sup>1</sup>Department of Radiology, Massachusetts General Hospital, 55 Fruit St., Boston, MA 02150.

<sup>2</sup>Present address: Department of Radiology, Brigham and Women’s Hospital, Boston, MA 02115.

<sup>3</sup>Department of Radiology, Children’s Hospital of Philadelphia, 34th Street and Civic Center Blvd., Philadelphia, PA 19104. Address correspondence to D. Jaramillo (jaramillo@email.chop.edu).

<sup>4</sup>Department of Radiology, Children’s Hospital Boston, Boston, MA 02115.

<sup>5</sup>Department of Medicine, Massachusetts General Hospital, Boston, MA 02114.

<sup>6</sup>Department of Genetics, University of Alabama at Birmingham, Birmingham, AL 35294.

AJR 2005;184:962–968

0361–803X/05/1843–962

© American Roentgen Ray Society

## MRI of Neurofibroma in NF1

lesions, 33 had deep plexiform neurofibromas and 18 had subcutaneous neurofibromas.

Imaging evaluation of superficial neurofibromas has been limited. In the series by Ianicelli et al. [6], the sonographic appearance of subcutaneous neurofibromas was described as either platelike or possessing deep digitations. The appearance of these superficial lesions on MRI has not been well characterized, with only a few cases presented in the literature [7–9]. On the basis of these limited cases, superficial plexiform neurofibromas do not typically possess the targetlike appearance seen in their deep counterparts and can be easily mistaken for other entities, such as venous malformations [8].

Our hypothesis is that superficial plexiform neurofibromas are common and have MRI characteristics that are different from their deep counterparts; these lesions need to be recognized and differentiated from other superficial abnormalities. It is the goal of our study to evaluate the MRI characteristics of superficial plexiform neurofibromas in NF1 and to compare them to the characteristics of deep plexiform neurofibromas. This study is part of a multiinstitutional trial that we are conducting to determine the natural history of NF1, specifically by collecting growth data on plexiform neurofibromas. It is our goal to correlate these growth data with the MRI characteristics of deep and superficial neurofibromas. Ultimately, we hope to determine whether a faster rate of growth is associated with certain imaging characteristics. Imaging-based prognostic indicators are potentially a very useful tool and could be used to triage which patients should pursue more aggressive therapy or monitoring.

### Subjects and Methods

#### Patients

Sixty-six patients (age range, 2–54 years; median age, 15 years) with primarily superficial plexiform neurofibromas were compared with a similar group of 56 patients with deep plexiform neurofibromas (age range, 4–54 years; median, 12 years). Fourteen medical institutions, located worldwide, are collaborators in a study on the natural history of NF1 sponsored by our group. All patients with a diagnosis of NF1 were offered participation in our study by each of these institutions; the patients who volunteered were enrolled and imaged. Patients were eligible for enrollment only if they met established clinical criteria for NF1—that is, the presence of two or more of the following: café-au-lait macules, neurofibromas, Lisch nodules, axillary or inguinal freckling, optic glioma, distinctive osseous

lesions, or first-degree relative with NF1 [10, 11]. Because these clinical criteria are well established and widely accepted, pathologic confirmation of neurofibroma is not a requirement and is not routinely recommended for the diagnosis of NF1. As a result, pathologic correlation was not consistently available for all patients. Biopsy of lesions is usually reserved for cases in which the diagnosis of NF1 is in question because of equivocal clinical findings, or for lesions that are rapidly enlarging. It was not a goal of this study to diagnose plexiform neurofibromas on the basis of MRI but rather to characterize the MRI appearance of these lesions in patients with an established diagnosis of NF1.

MR images from each patient were sent to a central location from each of these institutions. Human research committee approval was obtained at each institution, and informed consent was obtained from all participants.

#### MRI

For all patients, contiguous axial STIR (TR/TE, 6000/35; inversion time, 150 msec; echo-train length, 8) images and coronal or sagittal STIR images were obtained. STIR is a fluid-sensitive, fat-suppressing sequence that was chosen for the imaging protocol because of the very bright signal characteristics of neurofibromas relative to surrounding muscle, fat, and bone. Contrast-enhanced imaging was not performed for two main reasons: first, Ianicelli et al. [6] showed that plexiform neurofibromas are consistently bright in T2 signal intensity and therefore are very conspicuous on STIR and other T2-weighted sequences. In addition, they found that plexiform neurofibromas show variable enhancement after IV gadolinium administration on T1-weighted sequences; therefore, their conspicuity on contrast-enhanced images is inconsistent. Because IV contrast material provides no gain in conspicuity of plexiform neurofibromas, it was decided that there was no justification for the added risk or expense of gadolinium-enhanced imaging in this group of voluntary subjects.

Because patients were referred as part of a multiinstitutional study, MRI was performed on scanners of different makes and field strengths, with 35 magnets at 1.5 T and one magnet at 1.0 T. Coil, slice thickness, and field of view varied according to the location and extent of the lesion. Slice thickness was 4 mm for the head and neck, 5 mm for the trunk, and 10 mm for the extremities. The extremities were imaged with a matrix of  $512 \times 160$ ; other anatomic locations were imaged with a  $256 \times 256$  matrix.

#### Image Analysis

One lesion in each patient was evaluated. If a patient had multiple lesions, only the largest of the lesions was evaluated. We defined superficial

neurofibromas as lesions arising between the skin and muscle fascia. We defined deep neurofibromas as lesions arising underneath the muscle fascia. Some lesions contained both deep and superficial components. When a lesion had a predominantly (> 50%) deep component with a smaller superficial component, the lesion was considered a deep neurofibroma. Similarly, when the lesion was predominantly superficial (> 50%), with a smaller deep component, it was considered a superficial neurofibroma.

Each lesion was categorized by one radiologist as either being superficial or deep. The location within the body of each neurofibroma was then noted by the same radiologist. Location was categorized into one of the following three categories: trunk (chest, abdomen, and pelvis), extremity, or head and neck.

Each lesion was then graded with regard to numerous characteristics. Ten patients were reviewed jointly by two radiologists to establish a grading system of these characteristics. The remaining 112 patients were reviewed by one radiologist. Subsequently, 50 of these 112 patients were reviewed independently by the second radiologist, because this was the number of examinations required to establish the level of interobserver agreement (i.e., kappa statistic).

Note was made of whether the lesion was unilateral, bilateral and symmetric, or bilateral and asymmetric. The patient's midline was used as the axis of symmetry. Lesions involving a single extremity were categorized as unilateral. In addition, it was noted whether the lesion extended to skin surface (Figs. 1 and 2) and whether superficial lesions extended deep in relation to the muscle fascia.

The border definition of each lesion was evaluated and categorized as poorly defined or well defined (Figs. 3A, 4A, 5, and 6A). Poorly defined margins were those with a wide zone of transition, greater than or equal to 5 mm, between lesion and normal surrounding tissue or lesions having margins with numerous small digitations, smaller than 5 mm in diameter. Well-defined borders were those with a narrow zone of transition, less than 5 mm.

The morphology of each lesion was categorized as fascicular–nodular versus diffuse. Fascicular–nodular lesions were those consisting of a collection of smaller components that were tubular or spherical or both (Figs. 4B and 7). Diffuse lesions were those that lacked any definable geometry (Fig. 8). For each neurofibroma that was fascicular–nodular in morphology, the largest fascicle or nodule within the lesion was identified, and then its diameter was measured using Cheshire image analysis software (Parexel).

The signal characteristics of each lesion were categorized as homogeneous, targetlike, or heterogeneous without targets (Figs. 3B, 6B, and 9). Tar-



**Fig. 1.**—10-year-old girl with superficial neurofibroma of knee. Sagittal STIR image (TR/TE, 6,000/35; inversion time, 150 msec; echo-train length, 8) shows skin involvement (arrow) located anterior to insertion of patellar tendon.

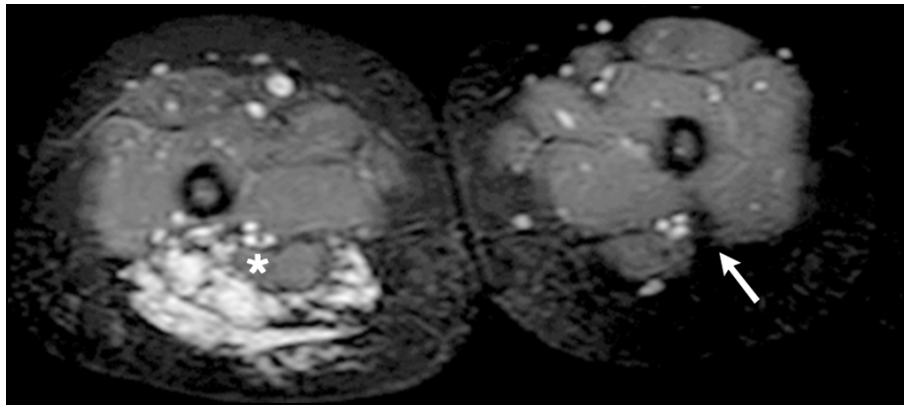


**Fig. 2.**—14-year-old girl with superficial neurofibroma of posterior right thigh without skin involvement. Axial STIR image shows that lesion abuts deep fascia and insinuates itself along lateral intermuscular septum but spares adjacent biceps femoris muscle (asterisk). Arrow points to normal position of lateral intermuscular septum on normal side.

getlike lesions are round, hypointense centrally, and hyperintense peripherally. Each lesion was evaluated for the presence of increased vascularity, as characterized by the presence of two or more flow voids (Figs. 9 and 10) that were increased in size or number or both compared with the normal side or with similar uninvolved regions of the affected side in cases in which the contralateral side was not imaged. Finally, the volume of each lesion was calculated using the Cheshire image analysis software, which uses a maximum-intensity-projection algorithm to define the borders of the lesion. The borders of each neurofibroma, as calculated by the software, were then confirmed by a radiologist (one for body lesions and another for head and neck lesions) before volume calculation was performed.

This additional review by the radiologist was necessary to exclude any T2 bright nonneurofibroma tissue inadvertently included by the software.

**Statistical Analysis**

We compared the MRI characteristics of deep and superficial neurofibromas. For categorical outcomes, chi-square tests were used to compare the statistical difference between outcomes. For continuous outcomes, mean or median was used to summarize the central tendency and Wilcoxon's rank sum tests were used to compare the distributions. The level of interobserver agreement (kappa statistic) was calculated on the basis of the 50 cases that had been reviewed independently by two radiologists. According to Landis and Koch [12], on the

basis of kappa values, agreement can be classified as almost perfect ( $\kappa = 0.81-1.00$ ), excellent ( $\kappa = 0.61-0.80$ ), good or moderate ( $\kappa = 0.41-0.60$ ), fair ( $\kappa = 0.21-0.40$ ), slight ( $\kappa = 0.00-0.20$ ), and poor ( $\kappa = 0.00$  or negative).

**Results**

A summary of the following results is presented in Table 1. There was no statistically significant difference in body location between the superficial and deep neurofibromas. Superficial neurofibromas were more likely than their deep counterparts to be unilateral (78% vs 55%) and less likely to be bilateral symmetric (7% vs 30%). Superficial neurofibromas were also more

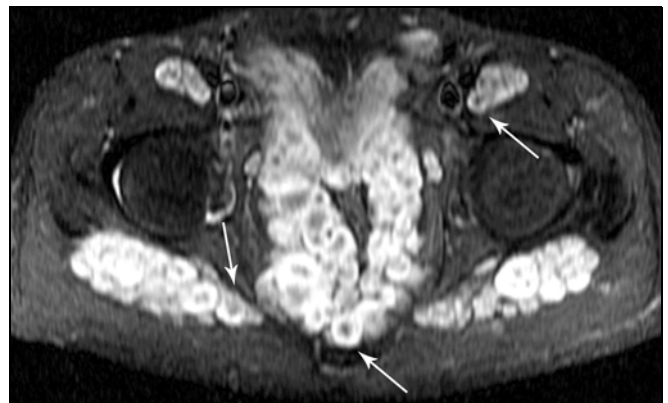


**Fig. 3.**—24-year-old man with deep, nodular neurofibroma of sciatic nerves in pelvis and gluteal region. **A**, Coronal STIR image shows well-defined borders (arrows). **B**, Axial STIR image shows targetlike (arrows) signal intensity.

## MRI of Neurofibroma in NF1

likely to extend to the skin surface (94% vs 40%). Of the superficial neurofibromas, 53% extended deep in relation to the muscle fascia.

Border definition (Figs. 3A, 4A, 5, and 6A) is poor with similar frequency (77% vs 68%) in the superficial and deep groups, respectively. Morphology (Figs. 4B, 7, and 8) of superficial neurofibromas was more likely to be diffuse (64% vs 11%). Of lesions that were fascicular or nodular in morphology, the superficial lesions had a smaller maximal fascicle-nodule mean diameter of 10.3 mm

than that of their deep counterparts (mean, 13.4 mm).

Signal characteristics (Figs. 3B, 6B, and 9) of superficial neurofibromas were infrequently targetlike (21%) and more likely to be homogeneous (35%) or heterogeneous without targets (44%); deep neurofibromas were more likely to be targetlike (75%) than homogeneous (4%) or heterogeneous without targets (21%). Superficial neurofibromas and deep neurofibromas exhibited increased vascularity (Figs. 9 and 10) with similar frequency (36% vs 48%).

The volume of the superficial neurofibromas was significantly smaller, with an average lesion volume of 180 cm<sup>3</sup> for superficial neurofibromas and 444 cm<sup>3</sup> for deep neurofibromas.

Subsequent MRI had been performed for 72 of our 122 patients, at follow-up intervals varying from 2 to 39 months. The rate of lesion growth was calculated for these patients in terms of both volume change and percentage of volume change over time. Although some of the lesions decreased in size, the overall pattern was one of lesion growth for both superficial and deep groups. The mean rate of volume growth for superficial neurofibromas was 18.7 cm<sup>3</sup>/year (median, 1.6 cm<sup>3</sup>; range, -185.0 to 399.1 cm<sup>3</sup>); for deep neurofibromas, it was 114.8 cm<sup>3</sup>/year (median, 25.8 cm<sup>3</sup>; range, -278.9 to 2,346.5 cm<sup>3</sup>) ( $p = 0.09$ ). The mean rate of percentage growth for superficial neurofibromas was 40.0% per year (median, 16%; range, -100% to 556%); for deep neurofibromas, it was 19.3% per year (median, 10%; range, -69% to 275%) ( $p = 0.68$ ).

Interobserver agreement ranged from very good to excellent for all the lesion characteristics evaluated, and simple kappa statistics ranged from 0.70 (excellent) to 1.0 (almost perfect). Levels of interobserver agreement are summarized in Table 2 [12].

## Discussion

Our study shows that superficial neurofibromas are more common than deep neurofibromas and have unique MRI characteristics. Superficial neurofibromas are usually unilateral or asymmetric and extend to the skin surface. They have diffuse rather than fascicular or nodular morphology, and the nodules and fascicles are smaller. Their signal characteristics are usually homogeneous or heterogeneous without targets. Superficial plexiform neurofibromas have a smaller average lesion volume than their deep counterparts, and their growth may be slower. Both superficial and deep neurofibromas have ill-defined margins and increased vascularity. When scanning a patient with NF1 on MRI, the radiologist should be aware that ill-defined, superficial lesions of high signal intensity on STIR or T2-weighted images are part of the NF1 spectrum and do not represent superimposed disease.

The targetlike MRI appearance of deep neurofibromas reflects their histologic composition. Woodruff [13] describes deep plexiform neurofibroma as microscopically consisting of a nerve or nerve fascicle distended by tumor cells, embedded in a rich

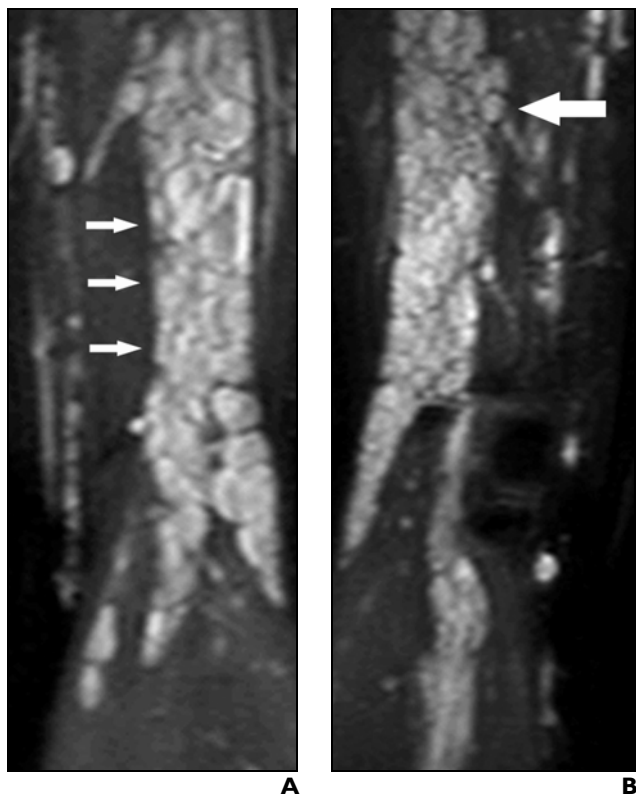


**Fig. 4.**—29-year-old woman with deep neurofibroma of leg. **A**, Coronal STIR image shows well-defined borders (*arrows*). **B**, Coronal STIR image shows nodular morphology (*arrow*).

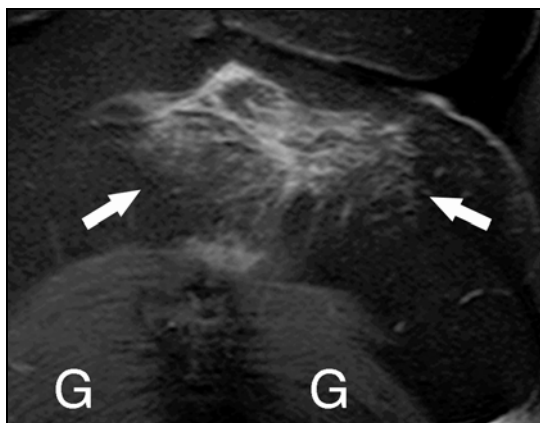


**Fig. 5.**—39-year-old woman with superficial neurofibroma of lower back. Coronal STIR image shows poorly defined borders (*arrows*). G = gluteal muscles.

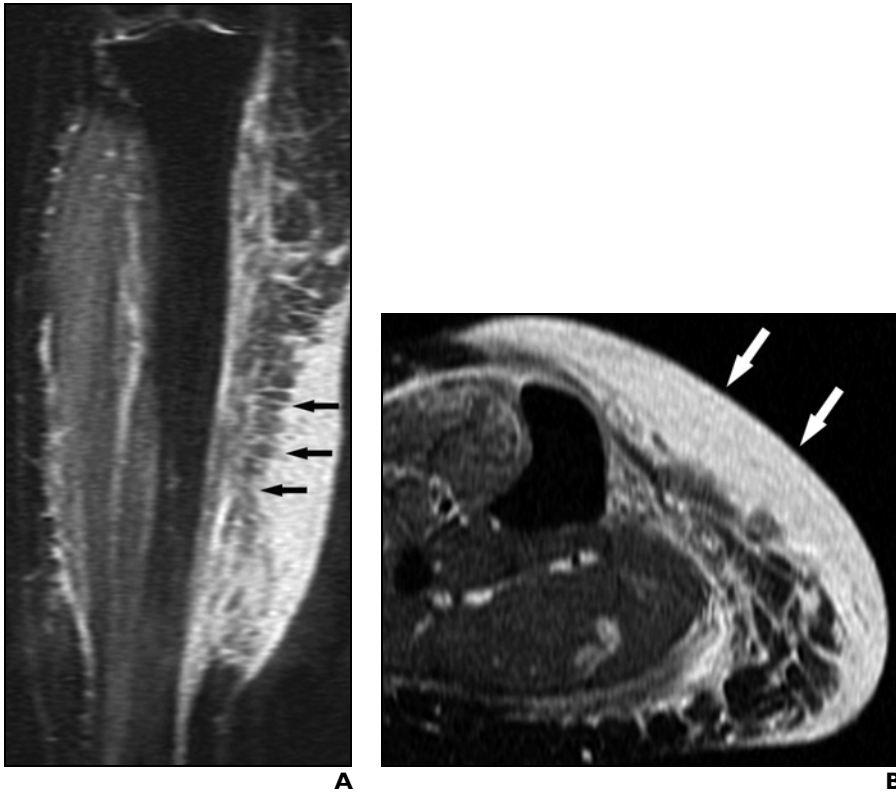


**Fig. 6.**—28-year-old woman with superficial neurofibroma of leg. **A**, Coronal STIR image shows poorly defined borders (*arrows*). **B**, Axial STIR image shows homogeneous signal intensity (*arrows*).



**Fig. 7.**—3-year-old boy with deep neurofibroma of thigh. Coronal STIR image shows that superiorly, there are numerous fascicles (*open arrow*) that divide distally into multiple branches (*solid arrows*).

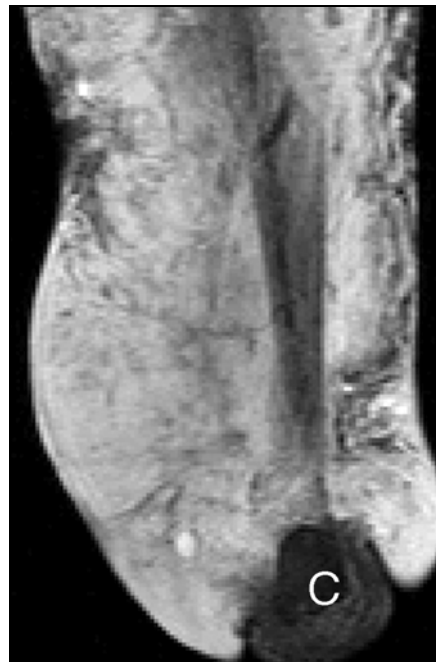


**Fig. 8.**—51-year-old woman with extensive superficial neurofibroma of leg. Coronal STIR image shows diffuse morphology. C = calcaneus.

myxoid matrix. Longitudinal bundles of residual nerve fibers are often centrally situated in the neurofibroma. This architecture could account for the centrally T2 dark (nerve fibers) and peripherally T2 bright (myxoid) appearance of these targetlike lesions [14, 15]. Woodruff [13] also described the histology of diffuse cutaneous and subcutaneous neurofibromas as spindle cells infiltrating around normal structures, such as skin adnexa, blood vessels, and adipose tissue. The ability of superficial neurofibromas to have poorly defined borders on MRI could be explained by this infiltrating microscopic architecture.

It is important to recognize the particular MRI characteristics of superficial neurofibromas for two main reasons. First, not all plexiform neurofibromas have the typical targetlike appearance. The absence of the targetlike appearance should not speak against a lesion being a neurofibroma, particularly if the lesion has a superficial location. In addition, it is important to consider neurofibromatosis as a differential diagnostic possibility when encountering an infiltrating, branching, high-signal-intensity lesion. These lesions may closely resemble a lymphatic or venous malformation, a hemangioma (when there are multiple associated flow voids), or, less commonly, a traumatic or inflammatory lesion of the subcutaneous tissues (Fig. 11).

One limitation of this study is that for reasons described in Subjects and Methods, we did not evaluate whether there is a difference in the contrast-enhanced appearance of deep versus superficial plexiform neurofibromas. Although Iannicelli et al. [6] reported inconsistent enhancement in their series of 46 patients, it may be of future interest to gather additional data regarding contrast enhancement of these lesions to determine whether the pattern of enhancement has any relationship to their biologic behavior. The existence of such a relationship is suggested by Mautner et al. [16], who described three asymptomatic NF1 patients with inhomogeneously enhancing plexiform neurofibromas on MRI. All three of these lesions were in fact shown to be malignant peripheral nerve sheath tumors.

The therapeutic options for superficial neurofibromas are limited. Surgical management offers limited benefit, particularly for superficial small, asymptomatic neurofibromas [17]. It is currently impossible to predict which small neurofibromas will eventually grow and invade surrounding tissues and which will remain stable in size.

## MRI of Neurofibroma in NF1

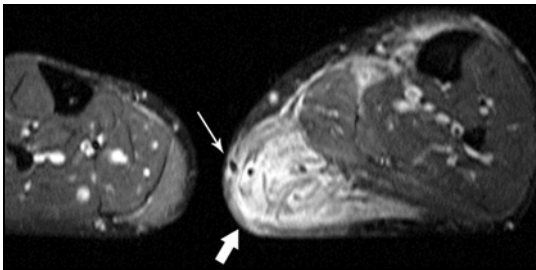


**Fig. 9.**—54-year-old man with superficial neurofibroma of calf. Axial STIR image shows heterogeneous signal intensity (*large arrow*). Flow voids are seen within lesion (*small arrow*).

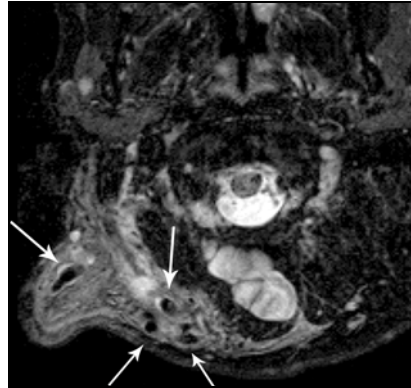


**Fig. 10.**—33-year-old man with superficial neurofibroma of right posterolateral neck. Axial STIR image shows multiple flow voids (*arrows*) consistent with blood vessels.

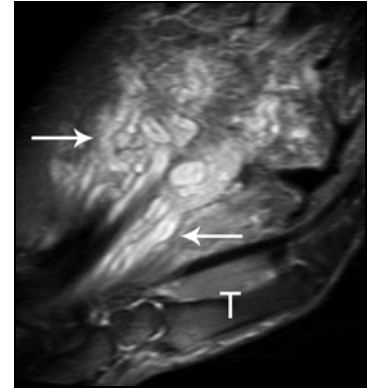


**Fig. 11.**—18-year-old man with deep neurofibroma of hand. Coronal STIR image shows multiple serpentine structures (*arrows*) resembling vascular malformation. T = thumb.

**TABLE 1** Summary of Results

Neurofibroma Characteristic	Superficial (n = 66)	Deep (n = 56)	p
Location in body			0.36
Head, neck	39%	36%	
Trunk	33%	39%	
Extremities	27%	25%	
Symmetry			0.004 <sup>a</sup>
Unilateral	78%	55%	
Bilateral asymmetric	15%	15%	
Bilateral symmetric	7%	30%	
Extension to skin surface	94%	40%	< 0.001 <sup>a</sup>
Extension deep to muscle fascia	53%	NA	NA
Border definition			0.31
Well-defined	23%	32%	
Poorly defined	77%	68%	
Morphology			< 0.001 <sup>a</sup>
Fascicular–nodular	36%	89%	
Diffuse	64%	11%	
Maximum fascicle–nodule diameter (mm)			0.013 <sup>a</sup>
Mean	10.3	13.4	
Median	8.0	11.5	
Range	3–37	4–33	
MRI signal characteristics			< 0.001 <sup>a</sup>
Homogeneous	35%	4%	
Targetlike	21%	75%	
Heterogeneous without targets	44%	21%	
Increased vascularity	36%	48%	0.20
Lesion volume (cm <sup>3</sup> )			0.002 <sup>a</sup>
Mean	180	444	
Median	72	193	
Range	1–1,640	1–3,849	

Note.—NA = not applicable.

<sup>a</sup>If  $p < 0.05$ .

Growth of plexiform neurofibromas can occur at any time in life. Periods of more rapid growth and development of new lesions have been observed in early childhood, during puberty, and during pregnancy. However, the overall growth pattern of plexiform neurofibromas is unpredictable, and even when untreated, spontaneous periods of stability or remission can occur. It is not known whether the location, histology, or radiologic appearance of a plexiform neurofibroma has any relation to its growth pattern. We hope that the study of the natural history of these lesions will help in understanding these questions. Our preliminary results based on 72 patients with follow-up imaging do not show a statistically significant different growth rate between deep and superficial neurofibromas, although the  $p$  value approaches statistical significance ( $p = 0.09$ ) for the change in lesion volume over time. It is our hope that as we acquire more data points, this relationship will become better understood.

This was a multiinstitutional study; therefore, there is variation in the technical factors and the

**TABLE 2** Interobserver Agreement

Lesion Characteristic	$\kappa$	95% CI
Symmetry	0.91	0.80–1.00
Extension to skin surface	1.0	
Extension of superficial lesions deep to muscle fascia	0.86	0.67–1.00
Border definition	0.70	0.49–0.92
Morphology	0.84	0.68–0.99
Signal characteristics	0.72	0.56–0.89
Increased vascularity	0.72	0.53–0.91

Note.—CI = confidence interval.

quality of the images. STIR imaging results in high signal intensity of slow-flowing vessels, which are difficult to differentiate from the neurofibromas. Plexiform neurofibromas are very complex lesions, and the categorization into superficial and deep lesions is somewhat arbitrary. Nonetheless, the signal characteristics of the superficial lesions are very different from those of their deep counterparts, and we believe that this classification identifies two groups of lesions that have different histology and possibly biological behavior. Histologic correlation is not available because, as described under Subjects and Methods, these lesions are not usually biopsied in patients with a clearly established clinical diagnosis of NF1. The data to show whether superficial and deep neurofibromas have different growth rates will not be available for several years. We hope to use these observations to further investigate the natural history of NF1, in the hope that imaging-based prognostic factors can be identified.

In summary, it is important to recognize that superficial plexiform neurofibromas have signal characteristics that differ from the typical targetlike lesions along the course of major nerves seen in deep plexiform lesions. Superficial plexiform neurofibromas in pa-

tients with NF1 are infiltrating lesions with diffuse morphology, asymmetrical distribution, and nontargetlike signal intensity; they have smaller fascicles and smaller volumes than deep plexiform neurofibromas.

#### References

1. Korf BR. Plexiform neurofibromas. *Am J Med Genet* 1999;89:31–37
2. Bhargava R, Parham DM, Lasater OE, et al. MR imaging differentiation of benign and malignant peripheral nerve sheath tumors: use of the target sign. *Pediatr Radiol* 1997;27:124–129
3. Suh JS, Abenzoza P, Galloway HR, et al. Peripheral (extracranial) nerve tumors: correlation of MR imaging and histologic findings. *Radiology* 1992;183:341–346
4. Varma DG, Mouloupoulos A, Sara AS, et al. MR imaging of extracranial nerve sheath tumors. *J Comput Assist Tomogr* 1992;16:448–453
5. McLaughran JM, Harris DI, Donnai D, et al. A clinical study of type 1 neurofibromatosis in northwest England. *J Med Genet* 1999;36:197–203
6. Iannicelli E, Rossi G, Almberger M, et al. Integrated imaging in peripheral nerve lesions in type 1 neurofibromatosis. *Radiol Med (Torino)* 2002;103:332–343
7. Beggs I, Gilmour HM, Davie RM. Diffuse neurofibroma of the ankle. *Clin Radiol* 1998;53:755–759
8. Peh WC, Shek TW, Yip DK. Magnetic resonance imaging of subcutaneous diffuse neurofibroma. *Br J Radiol* 1997;70:1180–1183
9. Jabra AA, Taylor GA. MRI evaluation of superficial soft-tissue lesions in children. *Pediatr Radiol* 1993;23:425–428
10. Gutmann DH, Aylsworth A, Carey JC, et al. The diagnostic evaluation and multidisciplinary management of neurofibromatosis 1 and neurofibromatosis 2. *JAMA* 1997;278:51–57
11. [No authors listed] Neurofibromatosis: conference statement—National Institutes of Health Consensus Development Conference. *Arch Neurol* 1988;45:575–578
12. Landis JR, Koch GG. The measurement of observer agreement for categorical data. *Biometrics* 1977;33:159–174
13. Woodruff JM. Pathology of tumors of the peripheral nerve sheath in type 1 neurofibromatosis. *Am J Med Genet* 1999;89:23–30
14. Kostelic JK, Haughton VM, Sether LA. Lumbar spinal nerves in the neural foramen: MR appearance. *Radiology* 1991;178:837–839
15. Kransdorf MJ, Moser RP Jr, Jelinek JS, et al. Intramuscular myxoma: MR features. *J Comput Assist Tomogr* 1989;13:836–839
16. Mautner VF, Friedrich RE, von Deimling A, et al. Malignant peripheral nerve sheath tumours in neurofibromatosis type 1: MRI supports the diagnosis of malignant plexiform neurofibroma. *Neuroradiology* 2003;45:618–625
17. Needle MN, Cnaan A, Dattilo J, et al. Prognostic signs in the surgical management of plexiform neurofibroma: the Children's Hospital of Philadelphia experience, 1974–1994. *J Pediatr* 1997;131:678–682

T. Thomas Zacharia  
Diego Jaramillo  
Tina Young Poussaint  
Bruce Korf

## MR imaging of abdominopelvic involvement in neurofibromatosis type 1: a review of 43 patients

Received: 29 April 2004  
Revised: 23 August 2004  
Accepted: 15 September 2004  
Published online: 27 October 2004  
© Springer-Verlag 2004

T. T. Zacharia  
Department of Radiology,  
Massachusetts General Hospital,  
Boston, MA, USA

D. Jaramillo (✉)  
Department of Radiology,  
Children's Hospital of Philadelphia,  
34th and Civic Center Boulevard,  
Philadelphia, PA 19104, USA  
E-mail: Jaramillo@E-mail.chop.edu  
Tel.: +1-215-5904842  
Fax: +1-215-5904318

T. Y. Poussaint  
Department of Radiology,  
Children's Hospital Boston, Boston, MA,  
USA

B. Korf  
Department of Genetics,  
University of Alabama at Birmingham  
Hospital, Birmingham, AL, USA

**Abstract Background:** Plexiform neurofibromas are a frequent complication of neurofibromatosis type 1. This article discusses MR imaging findings and distribution of plexiform neurofibromas in the abdomen and pelvis. **Objective:** To define the most prevalent patterns of involvement and MR imaging findings in abdominopelvic neurofibromatosis type 1. **Materials and methods:** We reviewed the MR appearance of abdominopelvic lesions in 23 male and 20 female patients (median age: 16 years) with type 1 neurofibromatosis. The patients were part of a multi-institutional study of 300 patients. Imaging included coronal or sagittal, and axial short tau inversion recovery images. **Results:** The most common abdominopelvic involvement was in the abdominopelvic wall ( $n=28$ , 65%) and lumbosacral plexus ( $n=27$ , 63%). Retroperitoneal involvement was

frequent ( $n=15$ , 35%). Lesions were less often intraperitoneal (21%) ( $P=0.001$ ). Pelvic disease ( $n=27$ , 63%), neural canal involvement ( $n=18$ , 42%), and hydronephrosis ( $n=4$ , 9%) were also noted. Target-like appearance of plexiform lesions was noted in more than half the patients. **Conclusion:** Abdominopelvic involvement in neurofibromatosis type 1 is primarily extraperitoneal. Although lesions are most prevalent in the abdominopelvic wall and lumbosacral plexus, retroperitoneal and pelvic involvement is common and usually affects important organs. MR imaging added information in the initial and follow-up clinical evaluation of these patients.

**Keywords** Neurofibromatosis type I · Plexiform neurofibromas · Abdominopelvic lesions · MR

### Introduction

Neurofibromatosis type 1 (NF1), an autosomal dominant disorder, has a highly variable natural history and phenotypic expression. Plexiform neurofibromas can cause significant morbidity because of disfiguring lesions, bone deformities, and involvement of adjacent structures. The risk of sarcomatous degeneration is low, between 3 and 5% [1, 2]. Malignant change typically occurs in young adults, with a male predominance [2].

Abdominopelvic involvement in NF1, although rare, can result in obstruction and dysfunction of the gastrointestinal tract and genitourinary tract. Sometimes these abdominopelvic symptoms can be the presenting findings in neurofibromatosis.

The MR imaging appearance of abdominopelvic neurofibromatosis has only been described in sporadic cases [3–5]. We report the findings in a series of 43 patients who are part of a larger cohort of nearly 300 patients with NF1 being studied within a multicenter trial

to determine the natural history of plexiform neurofibromas. In the subset with abdominopelvic involvement, our goals are to describe the major patterns of the tumors and to document the effects of neurofibromas on abdominal and pelvic structures.

## Materials and methods

### Subjects

We reviewed the MR appearance of abdominopelvic lesions in 23 male and 20 female patients, with a median age of 16 years (age range, 4–52 years). All patients fulfilled diagnostic criteria for NF1 [6]. The initial protocol was to have serial MR imaging examinations three times during a 3-year observation period. In our population, 21 patients have had one study, 19 have had two studies, and 3 have had three studies, for a total of 68 MR imaging examinations. The study is ongoing. As part of the plexiform neurofibroma multi-institutional study, MR imaging data of 300 patients were sent to a central location for analysis. Of these patients, 43 who had MRI scans of the abdomen were selected for analysis of abdominal lesions. The human research committees of the 14 participating institutions approved the study.

### MR imaging

All MR imaging was performed at high field strength, with 35 magnets operating at 1.5 T and one magnet at 1.0 T. Coil and field of view selection varied according to the location of the lesion. The protocol included coronal and contiguous axial short tau inversion recovery images (TR/TE 6,000/35; inversion time, 150 ms; echo-train length 8). Axial images were used for volumetric measurements. Slice thickness was 10 mm for the abdomen and pelvis. A 256×256 or 512×160 matrix was used. Contrast medium agent was not administered to any patient.

### Image analysis

Involved regions were classified as the abdominopelvic wall, nerve plexi, pelvis, and abdomen. Nerve plexus involvement was classified into sacral, lumbar, celiac, and para-aortic. Sciatic nerve involvement was noted in the lumbosacral plexus abnormalities, which were also graded based on their size. Lesions less than 1 cm in greatest diameter were classified as grade 0, those 1–5 cm as grade 1, and those greater than 5 cm as grade 2. Lesions were evaluated for the presence or absence of the typical target-like appearance, defined as a

well-circumscribed central area of low signal intensity and peripheral high signal intensity.

The affected abdominal and pelvic muscle groups were individually evaluated, and the frequency of involvement was studied for rectus abdominis, erector spinae, and gluteus. Genitourinary organs including the kidneys and ureter, the penis and scrotum in males, and the uterus in females were evaluated for patterns of involvement and for complications such as hydronephrosis and hydroureter. Secondary changes of the spine and pelvic bones such as neural foraminal widening, greater sciatic notch widening, and spinal cord compression were evaluated. Lesion signal intensity characteristics were analyzed. The serial progression of the tumor was quantitatively studied by volumetric analysis. Two radiologists jointly analyzed the images without knowledge of the patient's history or the rate of clinical growth, and graded the lesions by consensus.

### Statistical analysis

The significance of differences in prevalence of various findings was determined using the two-sample test of proportion (Intercooled Stata 7.0, Stata Corporation, College Station, TX, USA). A result with a *P* value less than 0.05 was thought to be significant.

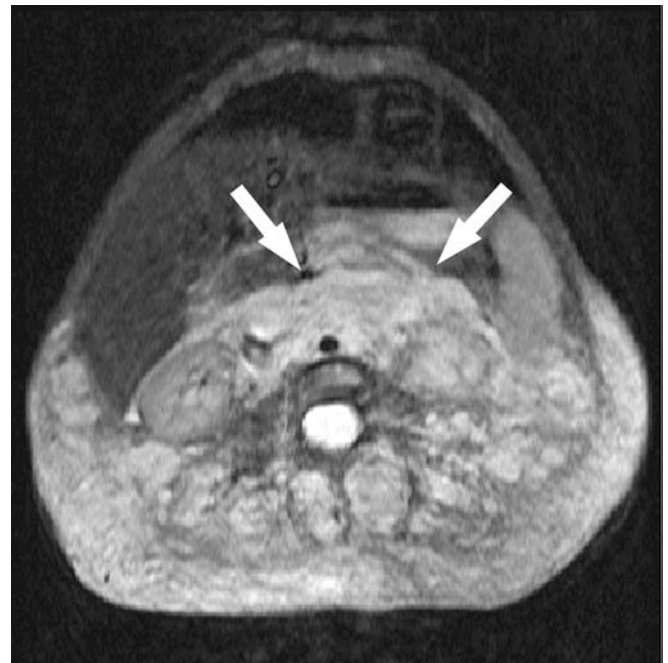
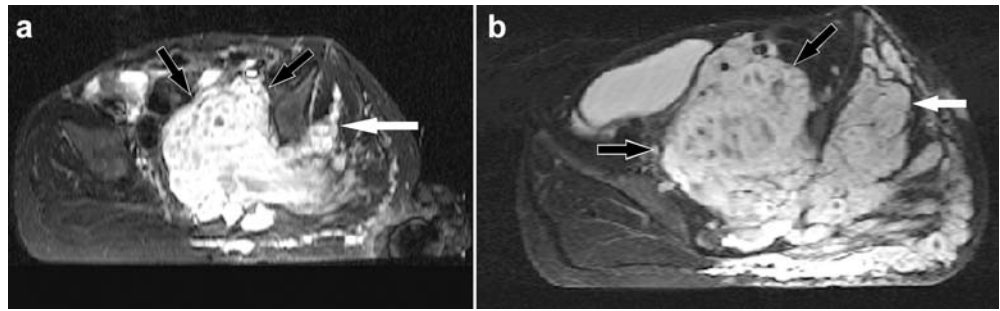


**Fig. 1** Axial STIR MR image (6,000/35) at the level of the kidneys shows posterior involvement of the abdominopelvic wall by a diffuse plexiform neurofibroma. Retroperitoneal involvement is also noted (arrows)

**Fig. 2** Axial STIR MR image (6,000/35) of the pelvis. **a** Plexiform neurofibromas involving the sacral plexus and left sciatic nerve (*black arrows*). Area of intramuscular involvement is noted on the left (*white arrow*). **b** Follow-up MRI after 3 years shows increase in the size of the lesions



## Results

The plexiform neurofibromas were primarily extra-peritoneal. The most common regions of involvement were the abdominopelvic wall ( $n=28/43$ ; 65% of patients), lumbosacral plexus ( $n=27/43$ ; 63% of patients), and pelvis ( $n=27/43$ ; 63% of patients). Abdominopelvic wall muscle involvement occurred primarily in the glutei ( $n=12$ ), iliopsoas ( $n=11$ ), and erector spinae ( $n=5$ ) muscles. This was because of the involvement of the nerve roots in the intermuscular planes. These lesions were predominantly hyperintense with areas of heterogeneity. Posterior abdominopelvic wall involvement ( $n=13$ ) (Fig. 1) was more frequently noted compared to anterior ( $n=7$ ) and lateral ( $n=8$ ) abdominopelvic wall involvement ( $P = 0.01$ ). Lumbosacral plexus ( $n=27$ ) involvement was combined lumbosacral ( $n=16$ ), isolated sacral ( $n=6$ ), or isolated lumbar ( $n=5$ ). In 17 patients, the involvement extended into the sciatic nerve

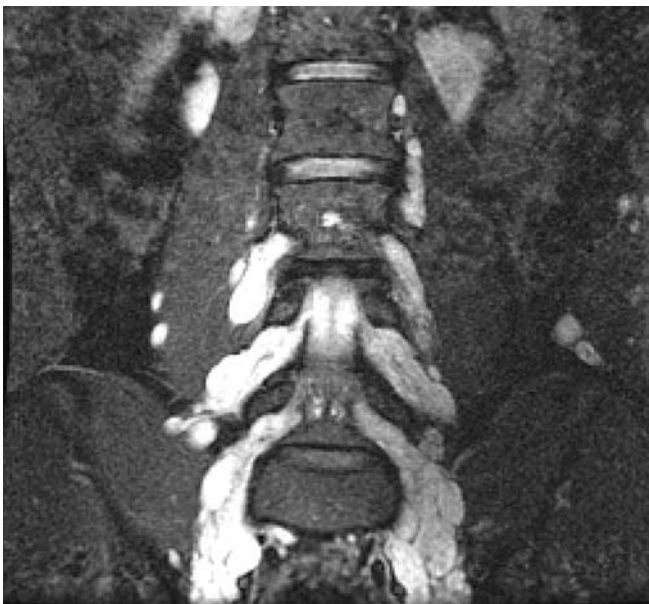


**Fig. 3** Coronal STIR MR image (6,000/35) shows extensive fusiform enlargement of the lumbosacral nerve roots

(Fig. 2). Lesions were either diffuse expansions of the nerve roots causing a chain-like appearance of nerves (Fig. 3) or large high signal intensity soft-tissue lesions causing mass effect on the surrounding abdominal structures, iliac vessels, sacrum, and iliac bones. Enlargement of sacral foramina was found in all 17 sciatic nerve lesions. Sciatic nerve tumors were also of high signal intensity and caused diffuse enlargement of the lower limb. Based on their size, lumbosacral plexus lesions were most commonly greater than 5 cm ( $n=17/27$ ), less often between 1 cm and 5 cm ( $n=9/27$ ), and seldom less than 1 cm ( $n=1$ ). Extension into iliopsoas ( $n=11$ ) and posterior abdominopelvic wall musculature was noted in cases of lumbar plexus involvement.

Pelvic lesions were either extensions of sacral lesions or primary lesions arising from the pelvic plexus of nerves ( $n=2$ ) causing perirectal invasion. Bladder involvement was noted in eight patients in the form of mass effect ( $n=1$ ) and diffuse or circumferential infiltration ( $n=7$ ). Genital involvement occurred in six patients, with involvement of the penis or scrotum ( $n=2$ ) and uterus or vagina ( $n=4$ ). A patient with vulvar neurofibroma demonstrated a large lesion with extension into the perirectal and periuterine region (Fig. 4).



**Fig. 4** Axial STIR MR image (6,000/35) at the level of the pubic symphysis shows hyperintense plexiform lesions involving the perirectal (*black arrow*) and labial region (*white arrow*). R rectum

Rectal involvement ( $n=13$ ) was noted in the form of mass effect ( $n=4$ ) and diffuse perirectal infiltration ( $n=9$ ).

Retroperitoneal lesions were distant from the lumbosacral plexus and originated from the autonomic plexus in the celiac and para-aortic region. The regions frequently involved were the para-aortic ( $n=12$ ), iliac ( $n=3$ ), and celiac ( $n=2$ ) regions. Diffuse celiac plexus involvement with infiltration into the peripancreatic region was noted in two patients. Hydronephrotic changes ( $n=2$ ) were a result of retroperitoneal nerve plexus involvement causing ureteric obstruction. The hydronephrosis was severe in one patient (Fig. 5) with significant renal enlargement and thinning of parenchyma.

Lesions were less commonly intraperitoneal ( $P=0.001$ ), being located in the mesentery ( $n=7$ ), spleen ( $n=1$ ), and liver ( $n=1$ ). Multiple plexiform lesions, which studded the mesenteric folds, were encountered in one patient, the hyperintense neurofibromas highlighted in the dark background of the visceral peritoneum on the STIR sequence (Fig. 6). The remaining six patients with mesenteric involvement had either focal primary mesenteric lesions ( $n=4$ ) or secondary lesions extending from the retroperitoneum ( $n=2$ ). Bony involvement included lumbosacral neural foraminal widening ( $n=20$ ), greater sciatic foramina widening ( $n=2$ ), and neural canal involvement ( $n=18$ ).

Target-like appearance was noted in 53% ( $n=23/43$ ) of patients. No subject showed loss of target-like appearance on follow-up imaging.

## Discussion

We have found that, in the abdomen and pelvis, plexiform neurofibromas primarily affect the abdominopelvic wall and retroperitoneal regions. Plexiform neurofibromas are a frequent complication of NF1 1 [7–10]. With the emergence of new treatment protocols for treatment

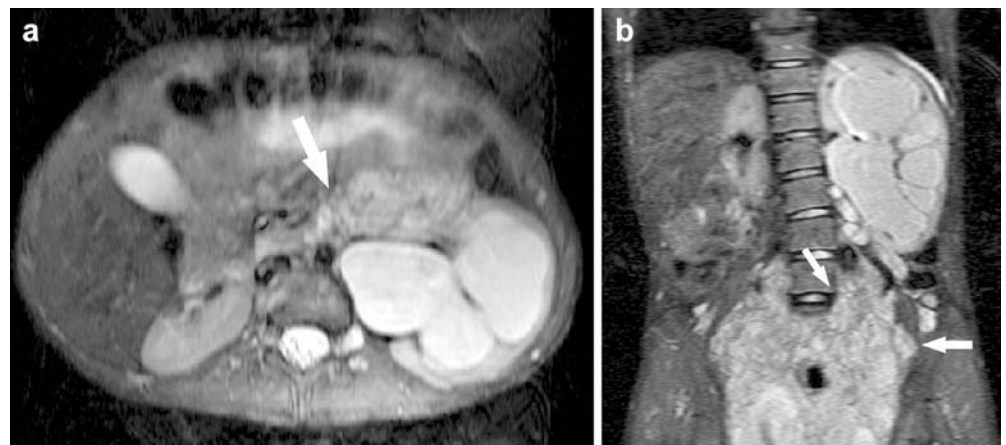


**Fig. 6** Coronal STIR image (6,000/35) shows plexiform neurofibromas (arrows) involving the mesentery. The classic target sign with central hypointensity and peripheral hyperintensity is seen

of plexiform neurofibromas [11], there is an increasing need to evaluate and classify these tumors.

Classification and analysis of complications of abdominal plexiform neurofibromatous lesions evaluated by MRI has not been reported. Abdominopelvic wall lesions are primarily posterior, probably because of the proximity of the posterior wall to the lumbosacral plexus and a lesser abundance of nerves in the anterior abdominopelvic wall. Lumbosacral plexus involvement resulted in significant secondary changes, such as spinal cord compression and obstructive hydronephrosis. Sacral plexus involvement produced mass effect on pelvic organs. Infiltration surrounding pelvic organs including the uterus and rectum was difficult to distinguish from primary involvement of the organ.

**Fig. 5** Retroperitoneal lesion causing hydronephrosis. **a** Axial STIR image (6,000/35); retroperitoneal neurofibromas (arrow) adjacent to the ureteropelvic junction. There is hydronephrosis of the left kidney. **b** Coronal STIR image (6,000/35). Retroperitoneal neurofibromas (arrows) causing ureteric obstruction and hydronephrosis of the left kidney



Autonomic plexus involvement was also found to be common. Liver and spleen neurofibromas are extremely rare [12]; we found only one case of each.

Abdominal plexiform disease distribution has been evaluated with CT but not with MR imaging. Bass et al. [13] described the CT appearances of abdominal lesions in NF1. They studied 16 patients and found that almost all had retroperitoneal plexiform neurofibroma with predominant involvement of the psoas major muscle. This agrees with our findings that extraperitoneal lesions were more common than intraperitoneal. Eight of their 16 patients had lumbosacral plexus lesions, similar to our experience ( $n = 27/43$ , 63%).

Biondetti et al. [14] emphasized the symmetric homogeneous appearance of paraspinal plexiform neurofibromas. Lumbosacral plexus tumors were asymmetric in 16 of 27 of our patients. Lesions were more likely to be symmetrical in the sacral plexus ( $n = 10$ ) than in the lumbar ( $n = 1$ ). The patients studied by Tonsgard et al. [2] had a high frequency of involvement of the sacral plexus, usually a result of a plexiform neurofibroma of the sciatic nerve that continued into the sacral plexus. Most of our patients also had predominant sacral plexus involvement with extension into the sciatic nerve ( $n = 17/22$ ). According to Tonsgard et al. [2], rectal and bladder involvement usually occurs by invasion by a large lesion. We found that in most cases, there was diffuse and intrinsic involvement of the walls of the bladder ( $n = 7/8$ ) and the rectum ( $n = 10/13$ ).

Retroperitoneal plexiform neurofibromas can cause complications such as mass effect on the spinal cord. We did not find any cases of sarcomatous degeneration. The small and large bowel can be affected by infiltration from retroperitoneal lesions, and these patients might present clinically with signs of bowel obstruction, but again, this was not seen. Ureteric obstruction and hydroureteronephrosis caused by retroperitoneal neurofibromas is a rare but important complication.

Huson et al. [8] studied the incidence of plexiform neurofibromas and found that 26.7% of individuals with NF1 had plexiform neurofibromas on physical examination. Tonsgard et al. [2] analyzed 126 individuals with NF1 using CT imaging and found an incidence of 20% in the thorax and 44% in the abdomen and pelvis.

Patients with plexiform neurofibromas can be asymptomatic when the lesions involve the viscera or the retroperitoneum. The clinical challenge and significance

lies in the diagnosis and serial evaluation for above-mentioned complications. Surgical resection is seldom performed because the tumor cannot be isolated from the nervous plexi. Surgery is performed primarily when there is a suspicion of malignant degeneration or when the lesion is disfiguring or incapacitating.

None of our patients had imaging evidence of malignant degeneration. MR imaging findings suggestive of degeneration include hemorrhage and necrosis [15] and loss of the target sign [16]. Clearly, patients presenting with masses of evidence of obstruction should be imaged. However, abdominal wall involvement, a common finding in NF1, is often an isolated abnormality and does not require further imaging. The timing of the follow-up imaging will be clarified when the data from the natural history of the disease become apparent. MR imaging is more valuable than CT studies because it delineates the imaging morphology and extent of these lesions better.

Treatment of plexiform neurofibromas in general remains a surgical challenge. Surgery is usually performed for cosmetic reasons and in lesions with rapid growth. When disfiguring lesions are operated on, patients remain recurrence-free for an average of 6.8 years [15]. Medical treatment using anti-angiogenic drugs and farnesyl transferase inhibitors is being evaluated [11]. The unpredictable natural history of these lesions causes challenges in treatment response evaluation.

This was a retrospective study, and although the cohort is relatively large, there is variability in the data. Despite a standardized protocol, there were substantial differences in coverage of the area.

In summary, abdominal and pelvic plexiform neurofibromas are significant because they often have serious clinical implications. Our study shows that abdominopelvic involvement in NF1 primarily affects the abdominopelvic wall and the lumbosacral plexus and less frequently the retroperitoneum and pelvis. MR provides good contrast definition between neurofibromas and the surrounding soft tissues and thus allows characterization of the extent of these lesions.

**Acknowledgments** We thank Meera Gupta, project manager, Susan Yan of Worldcare Inc. for help in the co-ordination of sites, and Noemi Chavez for help with the manuscript preparation. Supported by U.S. Army Grant No. NF70002, "Natural History of Plexiform Neurofibromas in NF1".

## References

1. Ducatman BS, Scheithauer BW, Piegras DG, et al (1986) Malignant peripheral nerve sheath tumors: a clinicopathologic study of 120 cases. *Cancer* 57:2006–2021
2. Tonsgard JH, Kwak SM, Short MP, et al (1998) CT imaging in adults with neurofibromatosis-1: frequent asymptomatic plexiform lesions. *Neurology* 50:1755–1760
3. Niku SD, Mattrey RF, Kalota SJ, et al (1995) MRI of pelvic neurofibromatosis. *Abdom Imaging* 20:176–178

4. Ros PR, Eshaghi N (1991) Plexiform neurofibroma of the pelvis: CT and MRI findings. *Magn Reson Imaging* 9:463–465
5. Topsakal C, Erol FS, Ozercan I, et al (2001) Presacral solitary giant neurofibroma without neurofibromatosis Type 1 presenting as pelvic mass—case report. *Neurol Med Chir (Tokyo)* 41:620–625
6. Neurofibromatosis (1988) Conference statement. In: National institutes of health consensus development conference. *Arch Neurol* 45:575–578
7. Enzinger FM, Weis SM (1995) Benign tumors of peripheral nerves. In: Gray SM, Gery L (eds) *Soft tissue tumors*, 3rd edn. Mosby, St. Louis, pp 1130–1132
8. Huson SM, Harper PS, Compston DA (1988) Von Recklinghausen neurofibromatosis. A clinical and population study in south-east Wales. *Brain* 111(Pt6):1355–1381
9. Riccardi VM, Kleiner B (1977) Neurofibromatosis: a neoplastic birth defect with two age peaks of severe problems. *Birth Defects Orig Artic Ser* 13:131–138
10. Sorensen SA, Mulvihill JJ, Nielsen A (1986) Long-term follow-up of von Recklinghausen neurofibromatosis. Survival and malignant neoplasms. *N Engl J Med* 314:1010–1015
11. Packer RJ, Gutmann DH, Rubenstein A, et al (2002) Plexiform neurofibromas in NF1: toward biologic-based therapy. *Neurology* 58:1461–1470
12. Imbert JP, Pilleul F, Valette PJ (2002) Value of MRI in hepatic plexiform neurofibromatosis. Case report. *Gastroenterol Clin Biol* 26:791–793
13. Bass JC, Korobkin M, Francis IR, et al (1994) Retroperitoneal plexiform neurofibromas: CT findings. *AJR* 163:617–620
14. Biondetti PR, Vigo M, Fiore D, et al (1983) CT appearance of generalized von Recklinghausen neurofibromatosis. *J Comput Assist Tomogr* 7:866–869
15. Korf BR (1999) Plexiform neurofibromas. *Am J Med Genet (Semin Med Genet)* 89:31–37
16. Lannicelli E, Rossi G, Almberger M, et al (2002) Integrated imaging in peripheral nerve lesions in Type 1 neurofibromatosis. *Radiol Med* 103:332–343



# NF1 plexiform neurofibroma growth rate by volumetric MRI

## Relationship to age and body weight

E. Dombi, MD; J. Solomon, PhD; A.J. Gillespie, RNMS; E. Fox, MD; F.M. Balis, MD; N. Patronas, MD; B.R. Korf, MD, PhD; D. Babovic-Vuksanovic, MD; R.J. Packer, MD; J. Belasco, MD; S. Goldman, MD; R. Jakacki, MD; M. Kieran, MD; S.M. Steinberg, PhD; and B.C. Widemann, MD

**Abstract—Objective:** To longitudinally analyze changes in plexiform neurofibroma (PN) volume in relation to age and body growth in children and young adults with neurofibromatosis type 1 and inoperable, symptomatic, or progressive PNs, using a sensitive, automated method of volumetric MRI analysis. **Methods:** We included patients 25 years of age and younger with PNs entered in a natural history study or in treatment trials who had volumetric MRI over  $\geq 16$  months. **Results:** We studied 49 patients (median age 8.3 years) with 61 PNs and a median evaluation period of 34 months (range 18 to 70). The PN growth rates varied among patients, but were constant within patients. Thirty-four patients (69%) experienced  $\geq 20\%$  increase in PN volume during the observation period. PN volume increased more rapidly than body weight over time ( $p = 0.026$ ). Younger patients had the most rapid PN growth rate. **Conclusions:** Volume increase of plexiform neurofibromas is a realistic and meaningful trial endpoint. In most patients plexiform neurofibroma growth rate exceeded body growth rate. The youngest patients had the fastest plexiform neurofibroma growth rate, and clinical drug development should be directed toward this population. Age stratification for clinical trials for plexiform neurofibromas should be considered.

NEUROLOGY 2007;68:643–647

Plexiform neurofibromas (PNs) in individuals with neurofibromatosis type 1 (NF1) are a major source of morbidity and, in some cases, undergo malignant transformation.<sup>1–3</sup> Surgery is the only standard treatment for PNs, but complete resection is difficult due to the large size and location of PNs, and regrowth of PNs after surgery is common.<sup>4,5</sup>

PNs may present at birth, and growth has been described as erratic.<sup>1</sup> An ongoing natural history

study of PNs in NF1 will provide data regarding the longitudinal growth of PNs using volumetric MRI analysis.<sup>1,6</sup>

Several agents have been evaluated in clinical trials for PNs.<sup>7,8</sup> The large size and complex shape of PNs, the limited understanding of their natural history, and their slow growth rate compared to solid cancers make quantitative evaluation of benefit from medical interventions challenging. Standard one- and two-dimensional solid tumor response criteria have limited value in detecting small changes in the size of PNs.<sup>9,10</sup>

Additional material related to this article can be found on the *Neurology* Web site. Go to [www.neurology.org](http://www.neurology.org) and scroll down the Table of Contents for the February 27 issue to find the title link for this article.

### Commentary, see page 627

This article was previously published in electronic format as an Expedited E-Pub on January 10, 2007, at [www.neurology.org](http://www.neurology.org).

From the Pediatric Oncology Branch (E.D., A.J.G., E.F., F.M.B., B.C.W.), NCI, Bethesda, MD; Medical Numerics, Inc. (J.S.), Sterling, VA; Diagnostic Radiology Department (N.P.), National Institutes of Health, Clinical Center, Bethesda, MD; University of Alabama at Birmingham (B.R.K.), Birmingham, AL; Mayo Clinic (D.B.-V.), Rochester, MN; Children's National Medical Center (R.J.P.), Washington, DC; Children's Hospital of Philadelphia (J.B.), Philadelphia, PA; Children's Memorial Hospital (S.G.), Chicago, IL; Children's Hospital of Pittsburgh (R.J.), Pittsburgh, PA; Dana Farber Cancer Institute (M.K.), Boston, MA; and Biostatistics and Data Management Section (S.M.S.), CCR, National Cancer Institute, Bethesda, MD.

This research was supported by the Intramural Research Program of the NIH, National Cancer Institute, Center for Cancer Research. This research was also supported by the U.S. Army through three clinical trial awards: 1) natural history of plexiform neurofibromas in NF1, grant no. NF70002; 2) phase II randomized, cross-over, double-blinded, placebo-controlled trial of the farnesyltransferase inhibitor R115777 in pediatric patients with neurofibromatosis type 1 and progressive plexiform neurofibromas, grant no. NF000027; 3) phase I/phase II study of pifenidone in NF1 and plexiform neurofibromas, grant no. NF010042.

Disclosure: The authors report no conflicts of interest.

Received March 21, 2006. Accepted in final form July 21, 2006.

Address correspondence and reprint requests to Dr. Eva Dombi, Pediatric Oncology Branch, National Cancer Institute, 10 Center Drive, Building 10 CRC, Room 1-5750, MSC 1101, Bethesda, MD 20892; e-mail: [dombie@mail.nih.gov](mailto:dombie@mail.nih.gov)

**Table 1** Equivalent percentage of change in diameter (RECIST), product of perpendicular diameters (WHO), and volume for spherical lesions (e.g., increasing the diameter of a sphere by 6% results in a 20% increase in the volume)

Percentage of change in tumor size		
RECIST diameter (1D)	WHO product (2D)	Ongoing NF1 studies volume (3D)
6	13	20*
12	25*	40
20*	44	73

\* The definition of progression according to the standard RECIST and WHO criteria, and the definition for progression by volumetric measurements used on several currently ongoing clinical trials for NF1-related plexiform neurofibromas. The volumetric method can more sensitively detect tumor progression.

RECIST = Response Evaluation Criteria in Solid Tumors; WHO = World Health Organization; NF1 = neurofibromatosis type 1; 1D = one-dimensional; 2D = two-dimensional; 3D = three-dimensional.

To more sensitively and reproducibly monitor the growth of PNs as the primary endpoint in clinical trials, we developed a method of automated volumetric MRI analysis of PNs.<sup>11</sup> This method has been used at the National Cancer Institute to centrally evaluate time to tumor progression in several multicenter trials for patients with NF1 and PN. In these trials, tumor progression is defined as a  $\geq 20\%$  increase in PN volume, a change that cannot be reliably detected with one- or two-dimensional measurements (table 1). In this study, we sought to

describe the growth rate of PNs and to analyze the relationship of tumor growth to age and body weight.

**Methods.** *Inclusion criteria.* Patients who were enrolled in one or more of several ongoing trials (table 2) were included in this study if they had NF1 and a measurable PN (longest diameter  $\geq 3$  cm), were 25 years of age or younger at the time of the first evaluation, had volumetric MRI analysis of their PNs at the Pediatric Oncology Branch between September 1999 and December 2005, had been followed with repeated MRI scans for a period of at least 16 months, and gave informed consent for serial MRI scans when enrolled in a clinical trial (table 2).

*Volumetric MRI method.* Axial and coronal short T1 inversion recovery (STIR) MR images were obtained to encompass the entire PN using a slice thickness of 5 to 10 mm with no skips between slices.<sup>6</sup> MRIs were performed at baseline, and then every 3 to 6 months for patients in treatment studies and every 6 to 24 months for patients in the NF1 natural history study. PN volume was determined as previously described using the MEDx software platform.<sup>11</sup> This method, which differs from the method used to measure PN volume in the current ongoing natural history study, is based on 1) contrast, defined by intensity in the tumor (high signal intensity) compared to the surrounding tissue (low signal intensity); 2) intensity gradient, defining the outside border (margin) of the lesion; and 3) size of the lesion. PNs are substantial in size, and small isolated areas of high signal intensity can be ignored because their contribution to the PN volume is insignificant. The steps of volumetric analysis are outlined in figure 1. This automated method is sensitive (detects volume changes as small as 10%) and reproducible (coefficient of variation 0.6 to 5.6%), and yields results similar to those of manual tumor tracings ( $R = 0.999$ ).<sup>11</sup>

When automated volume measurement was not feasible, the reason was recorded and manual tumor tracings using the drawing tool of the MEDx software were used to define tumor volume as previously described.<sup>11</sup>

*Data collection.* At each evaluation, patient age (years), weight (kilograms), and tumor volume (milliliters) assessed by automated or, if not applicable, manual volumetric MRI analysis as described above were recorded.

**Table 2** Use of automated volumetric (three-dimensional) MRI analysis of plexiform neurofibromas (PNs) in children and young adults with neurofibromatosis type 1 enrolled in multi-institutional clinical trials

Agent	Trial design	Eligibility for PN	Age, y	Trial endpoints	No.*	PI/trial status
Tipifarnib	Phase I	Inoperable	2–18	MTD, pharmacokinetics	3	F. Balis/completed
Tipifarnib/placebo†	Phase II, double-blind, placebo-controlled, crossover	Inoperable, progressive‡	3–25	Time to progression§	32	B. Widemann/ongoing
Pirfenidone†	Phase I	Inoperable	3–21	MTD, pharmacokinetics	10	R. Packer/completed
Pirfenidone†	Phase II	Inoperable, progressive‡	3–21	Time to progression§	10	R. Packer/ongoing
Peg-interferon alfa-2b†	Phase I	Inoperable, progressive, or symptomatic	1.5–21	MTD	2	R. Jakaacki/ongoing
—	Natural history	No current medical treatment for PNs	No limits	Growth rate of PNs	17	B. Korff/ongoing

\* Of 49 patients included in this report, 31 participated in one, 11 in two, and seven in three trials.

† Centralized volumetric MRI analysis of PNs from all patients is performed at the National Cancer Institute Pediatric Oncology Branch.

‡ Defined as  $\geq 20\%$  in three-dimensional,  $\geq 13\%$  in two-dimensional, or  $\geq 6\%$  in one-dimensional tumor measurements within approximately 1 year of trial entry or between the last two consecutive MRI studies.

§ Progression defined as  $\geq 20\%$  in tumor volume compared to baseline MRI.

MTD = maximum tolerated dose.

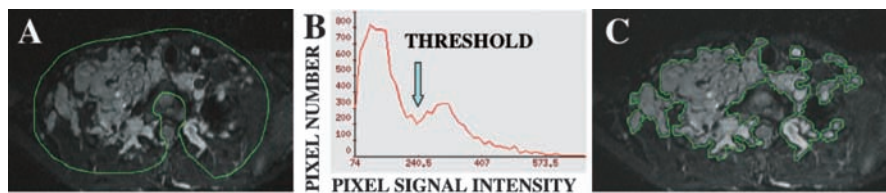


Figure 1. Steps of automated volumetric MRI analysis of plexiform neurofibromas (PNs): (A) Original axial short T1 inversion recovery MRI of a neck PN. The PN appears bright vs normal surrounding tissue. During the analysis, a region of interest including the tumor

and some low signal intensity surrounding tissue is manually outlined on each MRI slice. (B) The program derives a histogram of pixel signal intensity and identifies a threshold that separates the PN from surrounding tissue. (C) The program automatically defines the tumor contour.

**Data analysis.** PN volumes were calculated in milliliters. For patients who had more than one PN imaged, the volumes of the individual tumors were summed to obtain a total tumor volume and only time points with complete data were included. Tumor volume (milliliters) was converted to tumor weight (grams) using a density of one (1,000 mL = 1 kg). Changes in tumor volume, body weight, and tumor weight expressed as a percentage of body weight over time were calculated. PN growth and body growth rates were expressed as the percentage of change in tumor volume and body weight per year.

We performed two analyses to explore the relationship between tumor growth rate and increase in body weight of patients over time. 1) For each patient, tumor weight expressed as a percentage of body weight was plotted as a function of time since the initial MRI was performed. The resulting individual patient slopes, which were determined by linear regression, would be estimates of the change in tumor weight as a percentage of body weight. These slopes would be positive if the percentage of body weight made up of tumor were increasing over time and negative if the percentage of body weight made up of tumor were decreasing over time. The Wilcoxon signed rank test was used to determine whether there was a significant change in tumor weight as a percentage of body weight over time. If these slopes were centered on zero, this would indicate that there was no overall change over time in the percentage of body weight made up of tumor. 2) For each patient, linear regression was used to obtain the slopes for the percentage of change in tumor volume and percentage of change in body weight as a function of time since the initial MRI. If the percentage of change in tumor volume and body weight changed at the same rate, the ratio of the slopes would equal 1. The Wilcoxon signed rank test was used to determine whether the ratio centered around 1.

To analyze the relationship of age to PN growth rate and body growth rate, the percentage of change in tumor volume and the percentage of change in body weight per year were each plotted against the patient age. The relationship between PN growth rate and age was well described by fitting an exponential equation.

Finally, the Wilcoxon rank sum test was used to compare PN volume increase per year in children younger and older than the median age (8.3 years) at study entry.

All *p* values are two tailed.

**Results. Patient characteristics.** Fifty-six patients with NF1 and PNs had been followed with MRI for at least 16 months. We were unable to evaluate seven of the 56 patients in this study because of incomplete MRIs or inconsistent MRI coverage of the PN preventing longitudinal volumetric analysis (*n* = 4) or debulking surgery to the PN (*n* = 3). One of the seven unassessable patients also had evidence of a growing lesion within a stable PN. This raised suspicion of malignant degeneration, and the lesion was subsequently confirmed at surgery to be a low-grade malignant peripheral nerve sheath tumor. Thus, 49 patients with 61 PNs were included in this study. Eight patients had two and two patients had three PNs.

The median (range) age of the 49 evaluated patients was 8.3 years (3.3 to 25 years), 30 were male, and 19 were female. The diagnosis of NF1 in these patients was based on fulfilling the NIH Consensus Criteria.<sup>12</sup> Thirty-seven of these patients who had large, symptomatic PNs were eval-

uated at the National Cancer Institute Pediatric Oncology Branch. Twenty-eight (57%) of the 49 evaluated patients had measurable PN progression as defined in table 2 within 1 year prior to their first evaluation, as required by the clinical trial eligibility criteria. Patients were evaluated as part of their participation on the clinical trials outlined in table 2. In addition, two patients received treatment with thalidomide, not as part of a clinical protocol.

**Volumetric MRI analysis.** The median duration of follow-up with MRI was 34 months (range 18 to 70 months), the median number of MRI evaluations per patient was seven (range 2 to 14), and the median interval between MRI studies was 3.9 months (range 0.6 to 35.3 months). A total of 373 MRI studies were analyzed in the 49 evaluated patients. Automated volumetric MRI analysis was not feasible for eight patients due to artifacts resulting from spinal metal implants (*n* = 4) and lack of contrast between tumor and surrounding nontumor tissue (*n* = 4). For these patients, manual volume determinations were performed.

PN volumes expressed in milliliters and as a percentage of body weight at the start and end of the longitudinal observation period by patient, by PN, and by location of the PN are shown in tables E-1 and E-2 on the *Neurology* Web site at [www.neurology.org](http://www.neurology.org). Tumor burden was substantial in most patients (median PN volume at baseline 471 mL) and extreme in some patients, reaching up to 21% of body weight at baseline evaluation.

The growth of PNs over time in this longitudinal study was well documented using the volumetric MRI method. Overall, the PN volume increased by a median of 14.3% per year (table E-1), but this rate varied widely among patients (−3.1 to 68.3% per year). Over the course of the longitudinal observation period, PN volume increased by as much as 218%. There was no relationship between the PN growth rate and the site of the PN or the volume of the PN at baseline. Ten patients had more than one PN (table E-3). Among eight patients with two PNs, the median PN growth rate per year of the slower growing PN was 11.8% (range −3.6 to 63.6%), and the rate of the more rapidly growing PN was 25% (range 7.7 to 70.9%). In two patients with three PNs each, the PN growth rates per year ranged from 16 to 72% for Patient 9 and 12.9 to 18.4% for Patient 10 (table E-3).

**Relationship of PN growth rate and changes in body weight.** The percentage of change in tumor volume and body weight over time for the 49 evaluated patients is shown in table E-1 and figure 2A and B. During the evaluation period, 34 (69%) patients experienced ≥20% increase in PN volume, and 15 patients had less change in PN volume. The rate of PN growth varied among patients but

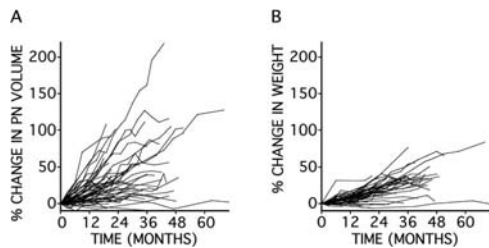


**Figure 2.** Percentage of change in plexiform neurofibroma (PN) volume (A) and body weight (B) over time in 49 patients with neurofibromatosis type 1 and PN.

appeared to be constant within patients. Erratic PN growth was not observed during the evaluation periods (figure 2A). Similarly, body growth appeared to be constant within most patients. The percentage of increase in body weight during the evaluation period was less than the percentage of increase in PN volume (table E-1, figure 2A and B).

The slopes resulting from the linear regression analysis of change in PN volume as a percentage of body weight over time were positive in 34 patients and negative in 15, indicating that PNs represented a greater proportion of body weight over time in most patients. The Wilcoxon signed rank test on the actual slopes had a two-tailed  $p$  value of 0.0015, indicating a tendency for PN volume (weight) to increase faster than body weight (and thus to represent a greater percentage of body weight) over time.

The relationship between the slopes representing the rate of PN growth and the rate of increase in body weight per year is shown in figure 3A. If the rate of PN growth equals the rate of increase in body weight, points will fall on the 45-degree line and the ratio of the slopes centers around 1. Thirty-three of the 49 patients (67%) had values above the 45-degree line, indicating that the PN volume increased more rapidly than the body weight. The Wilcoxon signed rank test of whether the slopes had a ratio that was equal to 1 had a two-tailed  $p$  value of 0.026. Thus, there was a tendency for the percentage of change in tumor volume over time to increase faster than the percentage of change in body weight over time in this population of patients, most of whom were selected for clinical trials based on demonstrated PN growth prior to enrollment.

**Relationship of PN growth rate and age.** The relationship between age and PN growth rate per year is shown in figure 3B. Younger children had a more rapid PN growth rate (percentage of change in PN volume per year) ( $R^2 =$

0.4), and in a subset of these patients, the PN volume increase per year exceeded 20%. For the ongoing clinical trials in patients with NF1 and progressive PNs, disease progression is defined as a 20% increase in PN volume from baseline. In the group of 49 evaluated subjects, there was also a tendency for patients younger than the median age of 8.3 years to have a greater increase in PN volume per year (median percentage of change per year 21.1% vs older children (median percentage of change per year 8.4%,  $p = 0.0010$  by the two-tailed Wilcoxon rank sum test). In contrast, the percentage of increase in body weight per year did not appear to be greater for very young children (figure 3C), but young adults, as expected, showed no increase in body weight over time. When PN growth rate is expressed relative to the rate of increase in body weight, PN growth still appears to be more rapid in younger children. Seventy-six percent (19/25) of children 8.3 years of age or younger had PN growth rate to the rate of increase in body weight ratios  $>1$  vs 58% (14/24) of patients older than 8.3 years, indicating that most young children had a PN growth rate exceeding the body growth rate.

**Discussion.** The clinical development of medical treatments for individuals with NF1 and PNs will depend on accurate measurement of the change in size of the PN over time to assess the effect of new treatments. However, the limited understanding of the natural history of PNs, their often large and complex shape, and relatively slow growth rate confound the accurate measurement of PNs. The natural history of PNs in NF1 is currently under study in a clinical trial,<sup>5,6</sup> and, as shown here, reproducible volumetric MRI methods for measuring PNs have been developed.<sup>6,11</sup> In addition, based on the expanding knowledge of the biology of PNs,<sup>5</sup> several novel targeted agents, which are under development for cancers and other diseases, have been identified as rationale agents for clinical evaluation in NF1, and these evolving imaging methods will likely serve as an important outcome measure in the clinical trials of new targeted agents.<sup>5,13</sup>

Our longitudinal study of volumetric MRI in patients with progressing PNs documents the variation in size and growth rate of PNs among patients, although some of this variability in growth rate could have been related to treatment effects in patients on one of several clinical trials. The PN growth rate

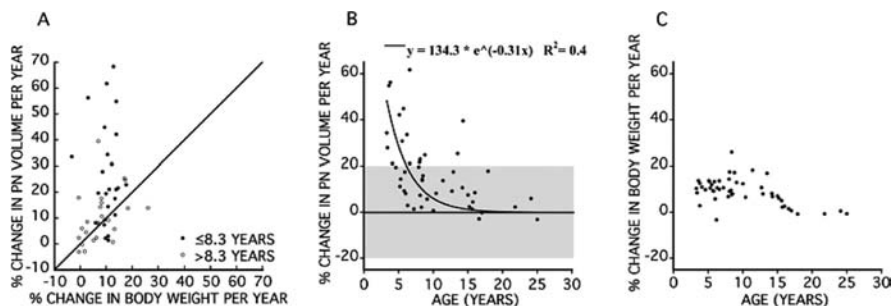


**Figure 3.** Relationship between the slopes for percentage of change in plexiform neurofibroma (PN) volume and percentage of change in body weight per year (A). Values above the 45-degree line represent ratios of the percentage of change in PN volume to the percentage of change in body weight that are  $>1$ . Closed symbols represent patients who are of or younger than the median age (8.3 years) at study entry, and open

symbols represent patients who are older than 8.3 years. Percentage of change in PN volume (B) and body weight (C) per year as a function of patient age at baseline. The shaded area indicates the 20% change in PN volume required for documentation of disease progression in ongoing clinical trials. The line in B represents an exponential fit to the data.

within each patient was constant rather than erratic, as previously thought.<sup>1</sup> However, the relatively short evaluation period (median 34 months) and the inclusion of predominantly young patients with symptomatic or progressive PNs limit this observation, and longitudinal volumetric analysis over more prolonged time periods is required to detect changes in PN growth rate as a result of hormonal or other influences.

This automated volumetric MRI analysis<sup>11</sup> was applicable to most PNs, and measurable growth of PNs could be detected in a substantial subset (69%) of patients within 1 year of the first evaluation. Volume increase of PNs therefore is a realistic and meaningful trial endpoint for patients with symptomatic or progressive PNs. However, longitudinal volumetric analysis is only possible if the entire PN is covered by the MRI study and if the same image acquisition protocol including STIR images is used consistently.

PN growth rate exceeded the rate of increase in body weight in most patients. The clinical impression that PNs grow faster in young children was confirmed in our study. We observed the most rapid PN growth rates in the youngest patients. The median age of patients at time of the first evaluation was 8.3 years (range 3.3 to 25 years), indicating that PNs become symptomatic or demonstrate progression at a young age, and the lower age limit of 3 years for participation in three of the clinical trials from which patients on this study came limited participation of even younger children. If effective, new treatments are more likely to prevent the growth of PNs rather than to reduce their size. Therefore, treatments are likely to be most effective if administered at the time of most rapid PN growth in young patients, and clinical drug development should be directed toward this population. In addition, based on the observation of more rapid PN growth rate in young children, consideration should be given to age stratification at trial entry in clinical trials for PNs.

In addition to documenting the natural history of PN growth and to serving as the primary outcome measure in clinical trials of new treatments for PNs, longitudinal volumetric analysis may also be useful for the detection of degeneration of PNs into malignant peripheral nerve sheath tumors. Identifying a change in PN growth rate or a growth rate that significantly exceeds the growth rates demonstrated here or by identifying significant growth of a compo-

nent within an otherwise stable PN may be potential indicators for malignant degeneration.

Progressive, symptomatic PNs in patients with NF1 are relatively uncommon, and randomized, placebo-controlled trials, such as the tipifarnib study described in table 2, may not always be feasible. Depending on the outcome of the ongoing clinical trials from which patients in this study were drawn, the data presented here may serve as a useful historical control population for future trials using volumetric MRI as the primary outcome measure.

Finally, it should be emphasized that the subjects in this analysis are a heterogeneous group, with subjects treated in several protocols with unknown effects on the natural history of PNs in NF1, including tipifarnib/placebo, pirfenidone, observation (natural history), or a combination of these. Thus, because of the heterogeneity and the fact that for patients in the randomized tipifarnib trial, their treatment assignment is still blinded, the results must be viewed somewhat cautiously and will require confirmation in a larger, more homogeneous group of patients before considering the results definitive.

## References

1. Korf B. Plexiform neurofibromas. *Am J Med Genet* 1999;89:31–37.
2. Korf BR. Malignancy in neurofibromatosis type 1. *Oncologist* 2000;5:477–485.
3. Evans DG, Baser ME, McLaughran J, Sharif S, Howard E, Moran A. Malignant peripheral nerve sheath tumours in neurofibromatosis 1. *J Med Genet* 2002;39:311–314.
4. Needle MN, Cnaan A, Dattilo J, et al. Prognostic signs in the surgical management of plexiform neurofibroma: the Children's Hospital of Philadelphia experience, 1974–1994. *J Pediatr* 1997;131:678–682.
5. Packer RJ, Gutmann DH, Rubenstein A, et al. Plexiform neurofibromas in NF1: toward biologic-based therapy. *Neurology* 2002;58:1461–1470.
6. Poussaint TY, Jaramillo D, Chang Y, Korf B. Interobserver reproducibility of volumetric MR imaging measurements of plexiform neurofibromas. *AJR Am J Roentgenol* 2003;180:419–423.
7. Gupta A, Cohen BH, Ruggieri P, Packer RJ, Phillips PC. Phase I study of thalidomide for the treatment of plexiform neurofibroma in neurofibromatosis 1. *Neurology* 2003;60:130–132.
8. Widemann BC, Salzer WL, Arceci RJ, et al. Phase I trial and pharmacokinetic study of the farnesyltransferase inhibitor tipifarnib in children with refractory solid tumors or neurofibromatosis type 1 and plexiform neurofibromas. *J Clin Oncol* 2006;24:507–516.
9. Therasse P, Arbuck S, Eisenhauer E, et al. New guidelines to evaluate the response to treatment in solid tumors. *J Natl Cancer Inst* 2000;92:205–216.
10. Miller AB, Hoogstraten B, Staquet M, Winkler A. Reporting results of cancer treatment. *Cancer* 1981;47:207–214.
11. Solomon J, Warren K, Dombi E, Patronas N, Widemann B. Automated detection and volume measurement of plexiform neurofibromas in neurofibromatosis 1 using magnetic resonance imaging. *Comput Med Imaging Graph* 2004;28:257–265.
12. National Institutes of Health Consensus Development Conference Statement: neurofibromatosis. Bethesda, Md., USA, July 13–15, 1987. *Neurofibromatosis* 1988;1:172–178.
13. Widemann BC. Merlin PAKs a punch. *Cancer J* 2004;10:8–11.